



RESEARCH ARTICLE

The influence of nutritional biological selenium nanoparticles (SeNPs) for controlling *Clinostomum marginatum* infection in Nile Tilapia (*Oreochromis niloticus*)

Haleema H. Albohiri¹, Muslimah N. Alsulami¹, Hayat S. Al-Rashidi², Mina A. Almayouf², Abeer Mogadem³, Asma A. Aljohani⁴, Haifaa A. Mahjoub⁵, Hind althagafi⁶, Mari Sumayli⁷, Suad Hamdan Almasoudi^{8*}, Ahmed Ezzat Ahmed^{9,10}

¹Department of Biological Sciences, College of Science, University of Jeddah, Jeddah, Saudi Arabia: ²Department of Biology, College of Science, Qassim University, Buraydah, Saudi Arabia: ³Department of Chemistry, College of Science, Taibah University, Madinah, Saudi Arabia: ⁴Department of Nutrition and Food Science, College of Science, University of Tabuk, UmLuj, Saudi Arabia: ⁵Biological Sciences Department, College of Science and Arts, King Abdulaziz University, Rabigh 21911, Saudi Arabia: ⁶Department of Biology, College of Science, Princess Nourah bint Abdulrahman University, P.O. Box 84428, Riyadh 11671, Saudi Arabia: ⁷Biology Department, College of Science, Jazan University, Jazan 82817, Saudi Arabia: ⁸Department of Biology, College of Sciences, Umm Al-Qura University, Makkah 21955, Saudi Arabia: ⁹Department of Biology, College of Science, King Khalid University, Abha 61413, Saudi Arabia: ¹⁰Prince Sultan Bin Abdelaziz for Environmental Research and Natural Resources Sustainability Center, King Khalid University, Abha 61421, Saudi Arabia

*Corresponding author: shmasuadi@uqu.edu.sa (Suad Hamdan Almasoudi)

ARTICLE HISTORY (25-663)

Received: July 12, 2025
Revised: August 31, 2025
Accepted: September 04, 2025
Published online: September 26, 2025

Key words:

Antiparasitic activity
Clinostomum marginatum
Gene expression
Growth performance
Nile tilapia
Selenium nanoparticles
(SeNPs)

ABSTRACT

Yellow grub (*Clinostomum marginatum*) infection severely impairs Nile tilapia productivity, causing growth retardation, hematological disorders, and increased susceptibility to secondary infections. This study comprehensively evaluates the biosynthesis, characterization, and multifaceted biological activities of selenium nanoparticles (SeNPs) produced using *Saccharomyces cerevisiae* SA33, which MALDI-TOF identified as *S. cerevisiae* DSM 34246 and their effect in mitigating infections caused by *Clinostomum marginatum*. The antioxidant, antibacterial, and antiparasitic activities of SeNPs were determined using the DPPH assay, disc assay, and measuring parasite mortality, respectively. UV-Vis spectroscopy confirmed the formation of SeNPs with a distinct absorption peak at 285 nm, and transmission electron microscopy (TEM) revealed well-dispersed, spherical nanoparticles with an average diameter of ~40 nm. Dynamic light scattering (DLS) and zeta potential analysis indicated a monodisperse size distribution (33 nm) and moderate colloidal stability (-22.35 mV). The biosynthesized SeNPs (200 µg/mL) exhibited potent dose-dependent antioxidant activity, scavenging over 90% of DPPH radicals. Antibacterial assay demonstrated significant growth inhibition against pathogenic bacteria. Antiparasitic activity of SeNPs against *Clinostomum marginatum* (Yellow Grub) reached >80% inhibition compared to praziquantel 75 %. In yellow grub-infected Nile tilapia, SeNPs (200 mg/kg diet) significantly enhanced growth performance, increasing final weight, weight gain, and feed efficiency, however, decreasing the FCR, while maintaining 100% survival. Hematological analysis of infected fish revealed SeNPs restored red blood cell counts, hemoglobin levels, and immune cell balance, counteracting parasitic anemia and inflammation. Serum biochemistry confirmed hepatoprotective effects, reducing stress markers (cortisol decreased from 9.89 to 1.90 µg/mL) and enhancing immune responses (lysozyme activity increased by 82%). Gene expression studies showed SeNPs upregulated growth-related genes (*GHR*) and myogenic regulators (*MYOG*, *MYF6*). Histopathological assessment demonstrated SeNPs' protective role, reversing gill damage (lamellar fusion, necrosis) caused by *Clinostomum* infection. Additionally, SeNPs reduced the bacterial count in water and fish organs. These findings highlight SeNPs as a versatile, eco-friendly nanomaterial with antioxidant, antimicrobial, antiparasitic, and growth-promoting properties, providing a sustainable solution for enhancing aquaculture health and productivity.

To Cite This Article: Albohiri HH, Alsulami MN, Al-Rashidi HS, Almayouf MA, Mogadem A, Aljohani AA, Mahjoub HA., Althagafi H, Sumayli M, Almasoudi SH, Ahmed AE, 2025. The influence of nutritional biological selenium nanoparticles (SeNPs) for controlling *Clinostomum marginatum* infection in Nile Tilapia (*Oreochromis niloticus*). Pak Vet J, 45(3): 1045-1060. <http://dx.doi.org/10.29261/pakvetj/2025.251>

INTRODUCTION

Aquaculture has become an indispensable component of global food security, accounting for nearly 50% of the world's fish supply for human consumption (FAO, 2022). Among cultured species, Nile tilapia (*Oreochromis niloticus*) ranks as the second most farmed fish worldwide due to its rapid growth rate, hardiness, and high market demand (Fitzsimmons, 2021; El-Saadony *et al.*, 2021a). However, parasitic infections remain a significant constraint to sustainable tilapia production, resulting in annual losses exceeding \$1 billion globally (Shinn *et al.*, 2023). The digenetic trematode *Clinostomum marginatum*, causative agent of yellow grub disease, has emerged as particularly problematic in tropical and subtropical aquaculture systems (Mahdy *et al.*, 2023).

Clinostomum marginatum infection manifests as characteristic yellow cysts in the muscle and gills of fish, leading to severe pathological consequences, including tissue necrosis, growth retardation, and increased susceptibility to secondary infections (Mahdy *et al.*, 2024a). Infected fish exhibit up to 40% reduction in growth performance and 30% mortality rates in commercial farms (Radwan *et al.*, 2023). The parasite's complex life cycle involving piscivorous birds as definitive hosts makes complete eradication challenging in open-water systems (Mwainge *et al.*, 2021). Current control strategies predominantly rely on chemical therapeutics such as Praziquantel and triclabendazole (Yildiz and Yilmaz, 2024). While effective, these compounds present significant drawbacks, including the development of parasite resistance (Mengarda *et al.*, 2023), negative impacts on non-target organisms (Caneschi *et al.*, 2023), and strict withdrawal periods that disrupt production cycles (Sedyaaw and Bhatkar, 2024). These limitations have spurred research into alternative control measures that are both effective and environmentally sustainable.

Nanotechnology has revolutionized disease management across multiple sectors, with particular promise for aquaculture applications (Mawed *et al.*, 2022; George *et al.*, 2023). Green-synthesized selenium nanoparticles (SeNPs) are produced through environmentally friendly methods, often utilizing plant extracts as reducing and capping agents, resulting in nanoparticles with enhanced biocompatibility and reduced toxicity compared to those synthesized by conventional chemical routes (Alqaraleh *et al.*, 2024; Ibrahim *et al.*, 2024). Characterization of green-synthesized selenium nanoparticles (SeNPs) from previous studies highlights their nanometer-scale size, negative surface charge, and functional activity. For selenium nanoparticles synthesized using *Euphorbia retusa* extract: TEM showed spherical particles below 100 nm; UV-Vis peak at 245 nm; zeta potential -19.0 mV; phytochemical contents (phenolics 82.71 mg gallic acid/g, flavonoids 15.64 mg catechin/g, tannins 4.73 mg tannic acid/g); antioxidant DPPH IC₅₀ of 0.247 mg/mL (Abduljabbara *et al.*, 2024; Ugli *et al.*, 2025). In another

study, SeNPs synthesized via *Pediastrum boryanum* extract had a TEM size range of 72.16–89.45 nm. FTIR analysis revealed capping by bioactives, and the antioxidant activity was lower compared to the extract (DPPH IC₅₀ not specified) (Al-Wakeel *et al.*, 2024).

SeNPs exhibit dose-dependent antioxidant activity by scavenging reactive oxygen species (ROS) (Freire *et al.*, 2024; Reda *et al.*, 2024), potent antimicrobial effects against fish pathogens (Qiao *et al.*, 2022), and immunomodulatory capabilities that enhance host resistance (Chen *et al.*, 2022). Their small size (10–100 nm) and high surface-to-volume ratio enable efficient cellular uptake and targeted action against parasites (Ifijen *et al.*, 2023). Selenium nanoparticles (SeNPs) exhibit remarkable antioxidant and antibacterial properties, making them particularly valuable in aquaculture. As potent antioxidants, SeNPs function by scavenging reactive oxygen species (ROS) and enhancing the activity of endogenous antioxidant enzymes such as glutathione peroxidase (GPx) and superoxide dismutase (SOD) (Khan *et al.*, 2023). This oxidative stress mitigation is crucial in fish exposed to parasitic infections, which induce excessive ROS production leading to tissue damage, immunosuppression, and growth retardation (Qiao *et al.*, 2022). Studies have demonstrated that dietary supplementation with SeNPs significantly reduces lipid peroxidation while improving total antioxidant capacity in fish tissues (Song *et al.*, 2021).

The antibacterial activity of SeNPs is equally noteworthy, with mechanistic studies revealing their ability to disrupt bacterial cell membranes, inhibit biofilm formation, and interfere with essential metabolic pathways in common fish pathogens, including *Aeromonas hydrophila* and *Staphylococcus aureus* (George *et al.*, 2023). Their broad-spectrum antimicrobial action helps prevent secondary bacterial infections that frequently complicate parasitic infestations in aquaculture settings. Beyond disease control, SeNPs play a pivotal role in enhancing growth performance and immunity in fish. At the molecular level, SeNPs upregulate growth-related genes (Ahmad *et al.*, 2022). This genetic modulation translates to measurable improvements in weight gain, feed conversion ratio (FCR), and specific growth rate (SGR) (El-Saadony *et al.*, 2021b).

Immunologically, SeNPs enhance both innate and adaptive immune responses by stimulating lysozyme activity, increasing immunoglobulin production, and promoting proliferation of lymphocytes and macrophages (Vijayaram *et al.*, 2025). These immunostimulatory effects are particularly valuable in parasitized fish, where SeNPs help restore compromised immune function while reducing cortisol-mediated stress responses (Sonsudin *et al.*, 2022). The dual functionality of SeNPs, which combat oxidative stress and pathogens while simultaneously promoting growth and immunity, positions them as a comprehensive solution for sustainable aquaculture productivity.

Previous studies have demonstrated the efficacy of SeNPs against various fish parasites, including

Ichthyophthirius multifiliis (Mahdy *et al.*, 2024b) and *Gyrodactylus turnbulli* (Martins and Santos, 2024). However, significant knowledge gaps remain regarding their specific effects against *Clinostomum marginatum* and comprehensive impacts on fish physiology. Most existing research has focused on *in vitro* assays or short-term *in vivo* trials without evaluating long-term growth performance, detailed hematological changes, or molecular mechanisms of action (Vijayaram *et al.*, 2025). Furthermore, comparative studies between SeNPs and conventional antiparasitic drugs remain limited, particularly regarding their relative effects on stress markers, immune function, and tissue repair processes (El-Saadony *et al.*, 2021b).

This study addresses these critical gaps through a multidisciplinary approach combining nanotechnology, parasitology, and fish physiology. Our specific objectives were to: (1) develop and characterize biosynthesized SeNPs using *Saccharomyces cerevisiae* DSM 34246; (2) evaluate *in vitro* antioxidant, antibacterial, and antiparasitic activities; (3) assess *in vivo* therapeutic efficacy against *C. marginatum* through comprehensive growth performance, hematological, and serum biochemical analyses; (4) elucidate molecular mechanisms via gene expression profiling of growth- and immune-related markers; and (5) compare SeNPs' effectiveness with conventional praziquantel treatment. The findings offer novel insights into sustainable parasite control strategies, advancing our understanding of nanomaterial applications in aquaculture health management.

MATERIALS AND METHODS

Isolation and identification of *Saccharomyces* species:

Saccharomyces spp. were isolated from the soil as follows: 10 g of representative soil samples were homogenized in 90 mL of sterile normal saline and shaken at 160 rpm for 30 minutes at room temperature (approximately 23 °C). Then, 0.1 mL of serially diluted samples was spread on yeast extract peptone dextrose (YPD) agar plates containing 100 mg/L chloramphenicol to prevent bacterial growth and different concentrations of sodium selenite (2, 4, 6, and 8 ppm), after incubating at 28 °C for two days. The colonies developed at the highest concentration of sodium selenite were selected for identification. The isolated strains were spotted on WL medium in duplicate and incubated at 28 °C for 5 days, after which the colony morphologies were observed. When the front side of the colony was cream with little green, raised and opaque, and the back side was white or with little green, it was initially considered as *S. cerevisiae* (Hu *et al.*, 2023). Then, the molecular identification of the isolated strains was performed by MALDI-TOF spectroscopy.

Synthesis and characterization of SeNPs: 0.1 g of *Saccharomyces* isolate was inoculated in 100 mL of Yeast Malt (YM) broth medium (Merck Co., Darmstadt, Germany) enriched with sterile sodium selenite (Na_2SeO_3) (Merck Co., Darmstadt, Germany) (8 mM) concentration, equivalent to 0.17 g of Na_2SeO_3 per 100 mL sterile YM broth medium (El-Sherbiny *et al.*, 2023), modified and incubated aerobically at pH 6, 32°C for 48 h on a shaker (IKA-KS 3000 control, Germany) at 120 rpm (Faramarzi *et*

al., 2020), modified. The color of the media begins to change simultaneously with yeast growth and eventually turns dark orange within the 48-hour incubation period. Confirmatory characterization of biogenic selenium nanoparticles was done using a UV-visible spectrophotometer (PG instrument, China T60U) at wavelengths ranging from 200 to 500 nm, TEM imaging—Transmission electron microscopy (Leo 0430; Leica, Cambridge, UK) to analyze the dimension and the structural aspects—morphology, shape, size, and distribution of biogenic Se-NPs. Se-NPs-rich yeast cells were eventually centrifuged twice using a laboratory centrifuge (SIGMA 2-16KL) at 5000 rpm at 25 °C for 2–5 minutes. After separation, all cells were rinsed three times with sterile deionized distilled water and centrifuged again under the same previously established conditions until further analysis (Faramarzi *et al.*, 2020).

Biological activities of SeNPs

Antioxidant activity: The DPPH scavenging activity of SeNPs was estimated by Alsulami and El-Saadony (2024) with some modifications. After adding 100 µL of ethanolic DPPH to 100 µL of SeNPs (25, 50, 100, 150, and 200 µg/mL) and incubating for 30 minutes in the dark, the resulting color was measured using a microplate reader (517 nm). The absorbance was incorporated into the subsequent equation.

$$\% \text{ DPPH scavenging activity} = (\text{Abs Control} - \text{Abs sample}) / (\text{Abs control}) \times 100 \text{ (1)}$$

Antibacterial activity: The antibacterial activity of SeNPs was evaluated against the following bacterial strains: *Aeromonas hydrophila* ATCC 35654, *Staphylococcus aureus* ATCC 6538, *Bacillus cereus* ATCC 11778, *Klebsiella pneumoniae* ATCC 13883, *Salmonella typhi* ATCC 14028, and *Escherichia coli* ATCC 11775. The bacterial strains were kept at 4 °C by subculturing them on nutrient agar slants. Alsulami and El-Saadony (2023) employed the agar well-diffusion method to evaluate the antibacterial activity of SeNPs. Following the addition of 50 mL of melted Muller-Hinton agar (MHA) to plates, a loopful of bacterial inoculum was distributed across the surface of each plate. Discs (8 mm) previously saturated with 50 µL of SeNPs at varying levels (25, 50, 100, 150, and 200 µg/mL) were applied to the surface of the MHA plates using forcips. The negative control was discs with ethanol, and the positive control was ciprofloxacin. For 24–48 hours, MHA plates were incubated at 37°C (Thagfan *et al.*, 2025). Diameters of the resulting inhibition zones (mm) indicated antibacterial activity compared to ciprofloxacin.

Antiparasitic activity: de Freitas Oliveira *et al.* (2021) evaluated the antiparasitic properties of SeNPs using the following methodology: *Clinostomum marginatum* cultures (density: 1×10^7 parasites/mL) were distributed into 96-well plates. The wells were treated with SeNPs at concentrations of 25, 50, 100, 150, and 200 µg/mL and incubated for 24 hours at 28°C. Post-incubation, resazurin reagent was added to each well. The viability of the parasites was quantified via colorimetric analysis, with the results expressed as a percentage of parasite mortality.

Experimental design: A 360 monosex of the Nile tilapia fingerlings (7.08 ± 0.08 g) were used in the current study. The fish were transported to the experimental aquaria in tanks provided with oxygen. Immediately after arrival, the fish were placed in glass aquaria filled with dechlorinated water and supplied with continuous aeration by a central air blower. The fish received the basal diet for three weeks to adapt to the new environment. At the beginning of the experiment, fish were randomly assigned to 24 glass aquaria (eight groups, three replicates, 15 fish per replicate). The first group was control, T1, T2, and T3 were Nile tilapia fish treated with selenium nanoparticles (50, 100, and 200 mg/kg), T4 was praziquantel-treated fish, T5 was yellow grub infected fish, T6 was yellow grub infected and treated with Selenium nanoparticles at 200 μ g/kg, meanwhile, T7 was yellow grub infected fish and treated with the antiparasitic drug (200 μ g/kg). Each glass aquarium ($60 \times 30 \times 40$ cm) contained 60 L of water. For ten weeks, each group was fed its experimental diet twice a day (8:00 AM and 4:00 PM) until satiation, and daily feed consumption was recorded. Using aerated and dechlorinated water, one-third of each tank was replaced twice daily. The remaining feed and feces were siphoned with the changed water. The experimental parameters included a water temperature of 26-30°C, ammonia levels of less than 0.2 mg/L, a pH of 6.4, nitrite at 0 mg/L, total hardness of 144 mg/L, undetectable free chlorine, and total alkalinity of 120 mg/L. The lighting program was 12 hours of light and 12 hours of darkness. To challenge fish with *Clinostomum marginatum*, fish in T5, T6, and T7 were immersed in buckets containing 5 Liters of water with *Clinostomum marginatum* for 20 minutes. Then, the infected fish were placed in aquaria.

Sample collection: After ten weeks of feeding on experimental diets, the fish were anesthetized using 25 mg/L tricaine methane sulfonate (MS-222). Then, the fish were weighed individually to obtain the final weight. For assays requiring whole blood, three fish per group had their caudal vein blood drawn into EDTA. Blood was also collected in tubes without an anticoagulant for serum preparation (three fish per group). Then, samples were centrifuged at 3000 rpm for 15 minutes at 4°C to separate the serum, which was then frozen at -20°C until use. For gene expression analysis, gill samples were collected from three fish per group on Cellix-RNA Guard reagent (Cellixza Biotechnology Company, Egypt) and frozen at -20°C until use. For histological analysis, gill specimens were dissected from the same site (24 fish, three per group) and immediately fixed in a 10% neutral buffered formalin until analysis.

Growth parameters: As demonstrated below, the fish growth performance parameters were computed in accordance with Abu-Elala *et al.* (2021). The analysis of survival rate and mean survival time was conducted according to the method of Khalil and Nasr-Allah (2025).

Body weight gain (BWG)

$$= \text{Final body weight (FBW)}g - \text{Initial body weight (IBW)}g$$

$$\text{Weight gain rate (WG \%)} = \frac{\text{FBW} - \text{IBW}}{\text{IBW}} \times 100$$

$$\text{Feed conversion ratio (FCR)} = \frac{\text{Feed intake (g)}}{\text{BWG (g)}}$$

$$\text{Specific growth rate } \left(\frac{\text{SGR}}{\text{day}} \right) \% = \frac{100(\ln \text{FBW} - \ln \text{IBW})}{\text{No days}}$$

$$\text{Survival rate (SR \%)} = \frac{\text{No fish at the end of experiment}}{\text{No fish at the beginning of experiment}} \times 100$$

Hematological parameters: RBCs were counted microscopically using a hemocytometer after dilution with a normal saline solution (Satheeshkumar *et al.*, 2012). Hb content was determined using a commercial kit from Bio-Lab Diagnostics Ltd. (Mumbai, India). Microhematocrit capillary tubes, centrifuged at $14,800 \times g$ for three minutes, were used to measure HCT (Satheeshkumar *et al.*, 2012). Blood indices, including mean corpuscular volume (MCV), mean corpuscular hemoglobin (MCH), and mean corpuscular hemoglobin concentration (MCHC), were determined using standard formulae of Lee *et al.* (1998).

$$\text{MCV} = \left(\frac{\text{PCV}}{\text{RBC}} \right) \times 10$$

$$\text{MCH} = \left(\frac{\text{Hb}}{\text{RBC}} \right) \times 10$$

$$\text{MCHC} = \left(\frac{\text{Hb}}{\text{PCV}} \% \right) \times 100$$

The total leucocytic count was determined using a hemocytometer after dilution with 0.1% Leishman stain in 2% glacial acetic acid solution (Dacie and Lewis, 1980). For the differential leucocyte count, thin blood films were spread on clean microscope slides and then stained with Leishman stain. Cells were counted according to Houwen (2001) using a $\times 1000$ oil-immersion light microscope to estimate the percentages of heterophils, lymphocytes, monocytes, eosinophils, and basophils. The total platelet count was determined using a 1% ammonium oxalate solution (Dacie and Lewis, 1980).

Blood Sampling and Biochemical Analysis Protocol:

Blood samples (3 mL) were collected from the caudal vein using heparinized needles and immediately transferred to sterile Eppendorf tubes, which were maintained at 4°C. Samples underwent centrifugation (Sigma 3-30K, Germany) at 10,000 rpm for 5 minutes at 4°C to isolate serum. Biochemical parameters were quantified according to methodologies established by Al-Deriny *et al.* (2020) and Dawood *et al.* (2020), utilizing assay kits (Bio-Diagnostic Co., Dokki, Egypt). Absorbance measurements were performed colorimetrically using a BioTek Elx808 microplate reader (USA) at specified wavelengths. The following markers were measured: metabolic markers, including blood glucose (GLU), and hepatic enzymes, such as Alanine aminotransferase (ALT) and Aspartate aminotransferase (AST). Immune function, i.e., respiratory burst activity via nitro blue tetrazolium (NBT) assay and lysozyme (LYZ) activity, and endocrine profiling, such as cortisol, reproductive hormones: Testosterone, Progesterone, Follicle-stimulating hormone (FSH), and growth hormone (GH). This standardized protocol ensures precise assessment of metabolic, immunological, and endocrinological responses in experimental subjects.

Gene expression: Total RNA extraction, cDNA synthesis, and real-time PCR Three gill specimens per group were homogenized in 1 mL TriQuick reagent (Beijing Solarbio Science & Technology Co., Ltd, China) using a mechanical tissue homogenizer. Total RNA was extracted from each homogenate according to the manufacturer's protocol. RNA integrity was verified for each sample via 1% agarose gel electrophoresis. The yield and purity (A260/A280 ratio) of each RNA extract were quantified using a UV1100 spectrophotometer (TechComp, Hong Kong). First-strand cDNA synthesis was performed with 1 µg total RNA per sample using the RevertAid First Strand cDNA Synthesis Kit (Thermo Fisher Scientific, Lithuania). The concentration and purity of the resulting cDNA were further assessed on a NanoDrop spectrophotometer (Thermo Fisher Scientific, Lithuania). Primers were designed with the primer-BLAST tool and synthesized by BIONEER Inc. (Alameda, CA, USA) (see Table 1 for sequences). qPCR reactions (final volume: 25 µL) were performed with Maxima SYBR Green qPCR Master Mix (2×) and ROX solution (Thermo Fisher Scientific, Lithuania) on a StepOnePlus real-time PCR machine. Each reaction contained 8.5 µL nuclease-free water, 12.5 µL SYBR Green master mix, 1.5 µL each primer (10 µM), and 1 µL cDNA (≤500 ng/reaction). Cycling conditions were: initial denaturation at 95°C for 8 min; 40 cycles of 95°C for 15 s, 57°C for 30 s (*ghr*, *mstn*, *myog*) or 60°C for 30 s (*myf6*); and final extension at 72°C for 30 s. Specificity was confirmed by melting curve analysis (95°C for 15 s, 60°C for 1 min, 95°C for 15 s). For each gene, the number of technical replicates per PCR reaction was as follows: three for *mstn* and *myf6* (to ensure accuracy when lower-expressing genes are more sensitive to handling variability and stochastic error), and two for *ghr* and *myog*, which consistently showed robust expression and technical reproducibility across pilot runs. Elongation factor 1a (*ef1a*) was used as a reference gene for data normalization (Yang *et al.*, 2013). Gene expression was calculated using the 2-ΔΔCT method (Livak and Schmittgen, 2001).

Histological evaluation of gills: The skeletal gill specimens (three per group) were processed and examined according to Hussein *et al.* (2021). Briefly, specimens were gradually dehydrated, cleared, embedded in paraffin, and sectioned at a thickness of 5-7 µm using a rotary microtome. Two sections from each sample were mounted on glass slides and stained with Hematoxylin and Eosin (H&E) stain, then examined under a bright-field microscope with a camera. Six photos of fixed cross-section areas were taken from different fields of each slide, and the numbers of cells were counted using the "Cell Counter" option of the ImageJ software.

Bacterial count in water and fish organs: Fish tissue samples (including skin, gills, intestines, and muscle) and water were systematically collected from experimental

aquaria at four timepoints: weeks 2, 4, 8, and 10. All samples underwent standardized processing for microbiological analysis. Fish tissues (10 g aliquots) were homogenized in 90 mL of sterile peptone buffer (0.1%), followed by serial decimal dilution to 10⁻⁷. Similarly, water samples (10 mL) were mixed with 90 mL of sterile peptone buffer and diluted to a concentration of 10⁻⁷. Bacterial quantification employed culture-based enumeration according to established protocols. For total bacterial counts, 100 µL aliquots from appropriate dilutions were plated on Plate Count Agar (PCA) and incubated at 37°C for 24 hours (Saad *et al.*, 2021). *Aeromonas* quantification was performed using selective *Aeromonas* agar medium with identical incubation conditions (Sheir *et al.*, 2020). Colonies were identified by their characteristic dark green pigmentation and black centers. All results were expressed as log₁₀ CFU/mL for both water and fish samples.

Statistical analysis: The data were inspected for ANOVA assumptions, including the normality and homogeneity of variance. One-way ANOVA and LSD test were employed for normally distributed data. For non-normally distributed data, the Kruskal-Wallis test with pairwise comparisons was used. The statistical analyses were conducted using SPSS version 25 software (IBM Corporation, Armonk, NY, USA). The significance was set at a probability value (*P*) of less than 0.05 and data were reported as the mean ± standard error (SE).

RESULTS

Histology of *C. marginatum* metacercariae: Fig. 1A displays clearly defined internal compartments with densely packed nuclei, representing developing reproductive organs characteristic of mature metacercariae. Fig. 1B shows a more segmented internal architecture with distinct cellular arrangements, indicating advanced metacercarial development, preparing for the adult stage transition.

A total of five specimens were processed and analyzed to ensure a consistent and reliable morphological assessment. The specimens, viewed at a magnification power of 400x, exhibit the typical oval morphology, ranging in diameter from 2 to 3 mm, which is consistent with the literature descriptions of *C. marginatum* metacercariae. The internal structures show organized tissue development, including presumptive suckers, reproductive primordia, and parenchymal cells that will differentiate into adult organs upon reaching the definitive bird host. The histological preparations represent mature metacercariae ready for transmission to piscivorous bird hosts. The well-organized internal anatomy and complete encystment indicate these parasites have successfully established chronic infections and evaded host immune

Table 1: Gene-specific primers used in the current study

Gene*	Accession number	Primer sequence (5'-3')	Annealing temperature (°C)	Amplicon length (bp)
<i>Ghr</i>	NM_001279455.1	F: ACATCAATCCTGGGCGGTC R: TAGTGGGGAGCAGTTAGAAGACA	57	165
<i>mstn</i>	XM_003458832.5	F: AATGATGGCAACTGAACCTGAT R: CAAGGAGCGGATTCTGATGTG	57	217
<i>myog</i>	NM_001279526.1	F: GAGGAGCACGCTGATGAACC R: TGACGACGACACTCTGGGC	57	181
<i>myf6</i>	NM_001282891.1	F: TGGACGAGCAGGAGAAAACC R: CCTCACTGACTGCTGTCTGTT	60	223
<i>ef1a</i>	NM_001279647.1	F: CTTCAACGCTCAGGTCATCA R: ATCTTCTCAACCAGCTCGCT	61	120

*Gene abbreviations: growth hormone receptor (*ghr*), myostatin (*mstn*), myogenin (*myog*), myogenic factor 6 (*myf6*), elongation factor 1a (*ef1a*), forward (F), and reverse (R).

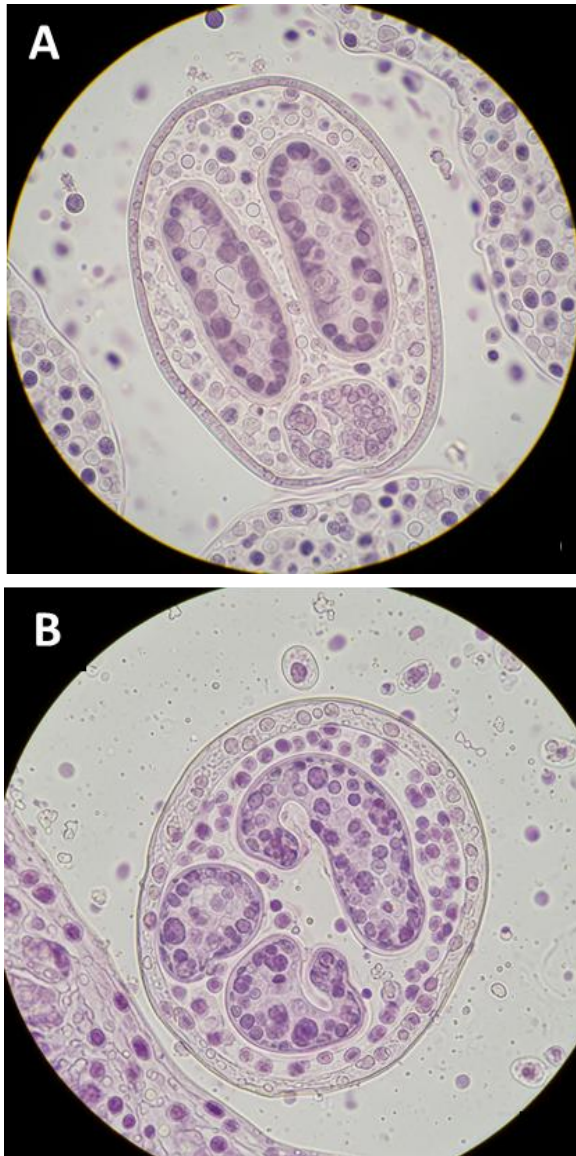


Fig. 1: Histological Sections of *Clinostomum marginatum* Metacercariae (400x) Showing Developmental Stages in Fish Tissue (A) mature metacercariae and (B) adult stage transition.

responses. The cellular differentiation patterns visible in both specimens suggest advanced metacercarial development with reproductive organs approaching maturity for the final transformation to adult trematodes in bird intestines.

Isolation and identification of *Saccharomyces* species:

Fifty *Saccharomyces* isolates were isolated from soil and coded as SA1 to SA50. Thirty isolates survived at 2 ppm sodium selenite, while 15 isolates survived at 4 ppm, 4 isolates at 6 ppm, and one isolate, SA33, survived at the highest concentration of sodium selenite (8 ppm). Based on microscopic and biochemical analysis, as well as Gram staining, it was identified as *Saccharomyces cerevisiae* SA33. This isolate was 99% similar to *Saccharomyces cerevisiae* DSM 34246 with a score value of 2.545, as determined by MALDI-TOF spectroscopy analysis.

Characterization of Selenium nanoparticles: Fig. 2 characterizes selenium nanoparticles (SeNPs) synthesized using *Saccharomyces cerevisiae* DSM 34246 through multiple techniques. The UV-Vis spectrum (Fig. 2A)

shows a sharp absorption peak at 285 nm. TEM images (Fig. 2B) reveal spherical, well-dispersed nanoparticles with uniform size and no significant aggregation. Dynamic Light Scattering (Fig. 2C) confirms a narrow, monodisperse size distribution centered around 33 nm, consistent with TEM observations. The zeta potential distribution (Fig. 2D) indicates a uniform surface charge near -22.35 mV, suggesting good colloidal stability.

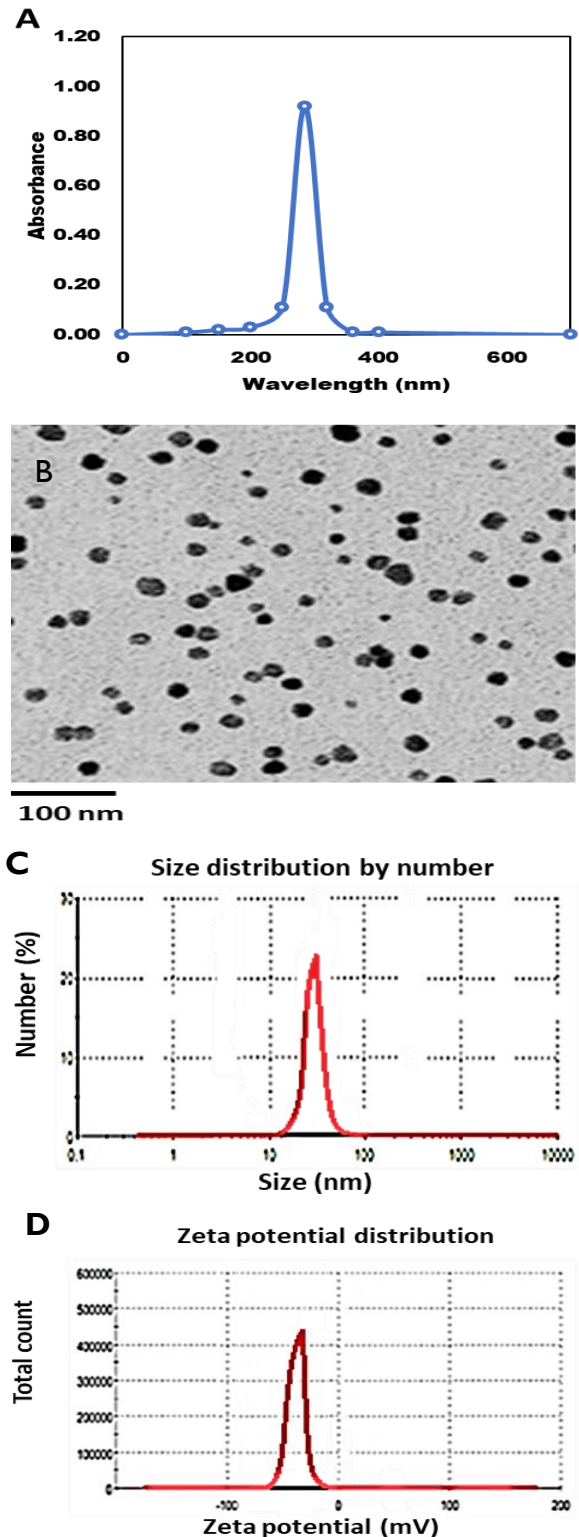


Fig. 2: Characterization of selenium nanoparticles fabricated by *Saccharomyces cerevisiae* DSM 34246 (A) UV absorbance at 285 nm, (B) TEM to detect the shape of SeNPs, (C) zeta sizer of SeNPs to detect the size, (D) zeta potential of SeNPs to detect the net charge.

Biological activities of SeNPs

Antioxidant activity of SeNPs: Fig. 3 clearly demonstrates a dose-dependent increase in the DPPH scavenging activity of the biosynthesized SeNPs. At the lowest concentration tested (25 µg/mL), the SeNPs exhibited approximately 45% DPPH scavenging activity. As the concentration of SeNPs increased to 50 µg/mL, the scavenging activity significantly improved to around 55%. Further increments in concentration to 100 µg/mL led to a substantial increase in antioxidant activity, reaching approximately 70%. At 150 µg/mL, the scavenging activity reached over 80%. SeNPs (200 µg/mL) exhibited considerable scavenging activity ($p < 0.05$), reaching over 90% compared to ascorbic acid at 91%.

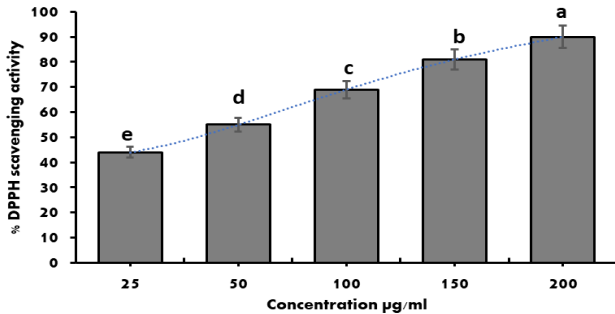


Fig. 3: Antioxidant activity of selenium nanoparticles fabricated by *Saccharomyces cerevisiae* DSM 34246 against DPPH free radicals.

Antibacterial activity of SeNPs: Increasing concentrations of selenium nanoparticles (SeNPs) led to progressively larger inhibition zones against all tested pathogenic bacteria, indicating a dose-dependent antibacterial effect (Table 2). At the highest SeNPs concentration (200 µg/mL), *Staphylococcus aureus* showed the largest inhibition zone (31 ± 0.6 mm); meanwhile, *Aeromonas hydrophila* and *Bacillus cereus* also exhibited substantial increases (26 ± 0.5 mm and 28 ± 0.6 mm, respectively) compared to ciprofloxacin with values of 30, 25, and 26, respectively. The MIC and MBC values were generally lowest for *Staphylococcus aureus* (0.28 ± 0.01 µg/mL and 0.48 ± 0.02 µg/mL, respectively), indicating

higher sensitivity to SeNPs; meanwhile, *Salmonella typhi* had the highest MIC and MBC ($0.48a \pm 0.02$ µg/mL and $0.88a \pm 0.03$ µg/mL), reflecting greater resistance compared to 0.30, 0.50, 51, and 0.90 µg/mL for ciprofloxacin (200 µg/mL). The negative control did not affect the bacterial strains.

Antiparasitic activity of SeNPs: Fig. 4 demonstrates a clear and statistically significant concentration-dependent increase in the inhibitory activity of SeNPs against *Clinostomum marginatum*. This indicates that these biogenic nanoparticles possess potent antiparasitic properties, which intensify with increasing concentrations. At the lowest tested concentration of 25 µg/mL, the SeNPs exhibited approximately 30% inhibition activity. As the concentration was progressively increased with a statistically significant dose-dependent increase in antiparasitic efficacy was observed. At 50 µg/mL, the inhibition percentage increased to over 40%. Further escalation to 100 µg/mL resulted in an inhibition activity exceeding. The efficacy increased, reaching nearly 70% at a concentration of 150 µg/mL. The highest concentration of SeNPs (200 µg/mL) achieved the maximum inhibition activity, surpassing 80%.

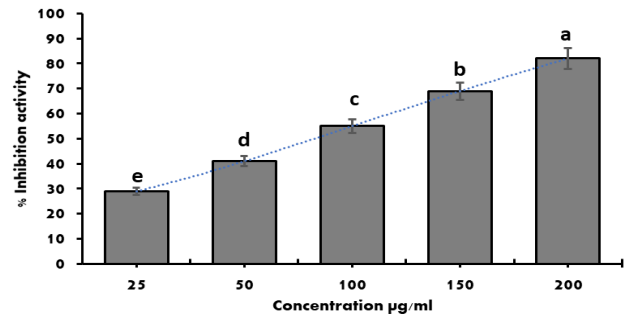


Fig. 4: Antiparasitic activity of selenium nanoparticles fabricated by *Saccharomyces cerevisiae* DSM 34246 against Yellow Grub (*Clinostomum marginatum*) expressed as inhibition percentage.

Growth performance of yellow grub-infected fish: Table 3 shows that growth performance reveals substantial improvements in Nile tilapia treated with selenium

Table 2: The inhibition zones diameters (mm) of SeNPs with MIC and MBC levels against pathogenic bacteria

Bacteria	SeNPs (µg/mL) / IZDs (mm)						MIC	MBC
	10	25	50	100	150	200		
<i>Aeromonas hydrophila</i>	14c ± 0.3	17bc ± 0.4	19b ± 0.5	21c ± 0.4	23c ± 0.5	26b ± 0.5	0.38b ± 0.02	0.68b ± 0.03
<i>Staphylococcus aureus</i>	17a ± 0.4	19a ± 0.4	22a ± 0.5	26a ± 0.5	28a ± 0.5	31a ± 0.6	0.28c ± 0.01	0.48c ± 0.02
<i>Bacillus cereus</i>	15b ± 0.3	18ab ± 0.4	20b ± 0.4	22b ± 0.5	25b ± 0.5	28b ± 0.6	0.33bc ± 0.02	0.58bc ± 0.02
<i>Klebsiella pneumoniae</i>	13c ± 0.3	15c ± 0.3	18c ± 0.4	21c ± 0.4	23c ± 0.5	25d ± 0.5	0.43ab ± 0.02	0.78ab ± 0.03
<i>Salmonella typhi</i>	10e ± 0.2	12d ± 0.3	15d ± 0.3	17d ± 0.4	19e ± 0.4	22f ± 0.5	0.48a ± 0.02	0.88a ± 0.03
<i>Escherichia coli</i>	11d ± 0.2	14cd ± 0.3	16cd ± 0.3	19d ± 0.4	21d ± 0.4	23e ± 0.5	0.43ab ± 0.02	0.78ab ± 0.03

Inhibition zones diameters (IZDs). Means in the same column with different lowercase letters are significantly different at $p \leq 0.05$. Values are presented as mean ± standard error (SE). Minimum inhibitory concentration (MIC), minimum bactericidal concentration (MBC).

Table 3: Growth performance of Nile tilapia (*Oreochromis niloticus*) fish infected with yellow grub (*Clinostomum marginatum*), and treated with selenium nanoparticles (SeNPs) and Praziquantel

Treatments	SeNPs (µg/Kg diet)	Antiparasitic agent	IW (g)	FW (g)	WG (g)	SGR (%/day)	TFI (g/fish)	FCR	SR (%)
Control	--	--	20.0 ^a ± 0.2	48.1 ^d ± 0.4	28.7 ^{cd} ± 0.3	0.52 ^c ± 0.01	35.0 ^d ± 0.6	4.8 ^{ab} ± 0.1	100.0 ^a
T1	50	--	20.5 ^a ± 0.3	55.0 ^c ± 0.6	34.5 ^c ± 0.5	0.7 ^a ± 0.01	51.0 ^{bc} ± 0.7	4.6 ^b ± 0.1	100.0 ^a
T2	100	--	19.8 ^b ± 0.2	57.0 ^b ± 0.7	37.2 ^b ± 0.6	0.7 ^a ± 0.01	52.0 ^b ± 0.8	4.0 ^d ± 0.1	100.0 ^a
T3	200	--	20.0 ^a ± 0.3	58.0 ^a ± 0.5	38.0 ^a ± 0.4	0.7 ^a ± 0.01	54.0 ^a ± 0.7	4.2 ^d ± 0.1	100.0 ^a
T4	--	200	20.0 ^a ± 0.2	55.0 ^c ± 0.6	35.0 ^{bc} ± 0.5	0.7 ^a ± 0.01	52.0 ^b ± 0.8	4.6 ^b ± 0.1	100.0 ^a
T5	--	--	19.4 ^b ± 0.3	45.0 ^d ± 0.5	25.0 ^d ± 0.4	0.5 ^b ± 0.01	47.0 ^c ± 0.5	5.0 ^a ± 0.1	89.9 ^b
T6	200	--	19.5 ^b ± 0.2	54.0 ^c ± 0.5	34.5 ^c ± 0.4	0.6 ^b ± 0.01	50.0 ^{bc} ± 0.6	4.5 ^b ± 0.1	100.0 ^a
T7	--	200	19.0 ^b ± 0.3	52.0 ^{cd} ± 0.6	33.0 ^c ± 0.5	0.6 ^b ± 0.01	48.0 ^c ± 0.7	4.3 ^c ± 0.1	100.0 ^a

Values with different superscript letters in the same column are significantly different ($P < 0.05$). IW = Initial Weight, FW = Final Weight, WG = Weight Gain, SGR = Specific Growth Rate, TFI = Total Feed Intake, FCR = Feed Conversion Ratio, SR = Survival Rate. The first group was control, T1, T2, and T3 were Nile tilapia fish treated with selenium nanoparticles (50, 100, and 200 mg/kg), T4 was praziquantel-treated fish, T5 was yellow grub infected fish, T6 was yellow grub infected and treated with Selenium nanoparticles at 200 µg/kg, while T7 was yellow grub infected fish and treated with the antiparasitic drug (200 µg/kg).

nanoparticles, particularly at 200 mg/kg (T3), compared to the uninfected control group. Specifically, fish in the T3 group exhibited a final weight of 58.0 g, representing a 28.9% increase over the control group (45.0 g). Weight gain in T3 reached 38.0 g, which is 52.0% higher than the control (25.0 g). The specific growth rate (SGR) improved by 40.0%, rising from 0.5%/day in the control to 0.7%/day in T3. Additionally, the feed conversion ratio (FCR) in the T3 group decreased by 12.5% compared to the control (from 4.8 to 4.2), indicating more efficient feed utilization. Survival rates (SR) remained at 100% in both groups, showing no change. Yellow grub-infected, untreated fish (T5) showed the poorest performance, with marked reductions in final weight, weight gain, and SGR, and an elevated FCR, highlighting the negative impact of yellow grub infection. Survival rates in T5 dropped by 10.1% compared to the control (from 100.0% to 89.9%). Praziquantel-treated groups (T4, T7) and SeNPs-treated infected fish (T6) showed intermediate improvements, but none matched the performance metrics of the T3 group.

Hematological Parameters of Yellow Grub-Infected Nile Tilapia Treated with SeNPs: Table 4 presents significant changes in blood parameters resulting from yellow grub infection and selenium nanoparticle (SeNPs) supplementation, highlighting the fish's physiological responses and recovery. The red blood cell count (RBCs) decreases sharply with infection (T5: $1.2 \times 10^6/\mu\text{l}$), indicating severe anemia, while SeNPs treatment improves RBCs dose-dependently, peaking at T3 ($2.3 \times 10^6/\mu\text{l}$), a 58% increase over controls. Hemoglobin levels follow a similar trend, with treated groups showing elevated concentrations (9.5–9.9 g/dL) compared to controls and infected, untreated fish (6.1 g/dL). Packed cell volume (PCV) is highest in infected fish (32.5%), likely reflecting dehydration rather than better oxygen transport, while SeNPs-treated groups maintain normalized PCV (27.2–28.2%). Infection causes larger, immature red blood cells with low hemoglobin content (MCV: 189 fl; MCHC: 22.9 g/dL), but SeNPs, especially at higher doses (T3, T4), promote smaller, mature erythrocytes with higher hemoglobin concentrations (MCHC: 32.5–33.5 g/dL), indicating improved blood quality. White blood cell counts rise substantially with infection ($39.7 \times 10^3/\mu\text{l}$), reflecting immune activation; however, SeNPs-treated infected groups show reduced counts ($22.3\text{--}23.6 \times 10^3/\mu\text{l}$), suggesting the resolution of inflammation. Elevated heterophils in infected fish decrease significantly with SeNPs treatment, indicating anti-inflammatory effects. Lymphocyte counts present

complex changes: infection increases their number, but SeNPs treatment in infected groups causes marked reductions, possibly signaling recovery or mild immunosuppression at high doses. Eosinophils appear only in infected, untreated fish, confirming parasitic infection, and are absent in all treated groups, demonstrating effective parasite control. Monocytes, elevated by infection, normalize with SeNPs supplementation, reflecting reduced tissue damage and repair needs.

Serum Biochemical Parameters, Immune Activity, and Hormone Levels:

Table 5 highlights clear physiological impacts of yellow grub infection and subsequent treatment in Nile tilapia. Infected, untreated fish (T5) showed severe liver dysfunction, with the highest glucose (127.0mg/dl) and elevated liver enzymes (ALT: 83.0U/l, AST: 153.0U/l), indicating significant stress and liver damage. Selenium nanoparticle (SeNPs) treatment, especially at 200 $\mu\text{g}/\text{kg}$ (T3), provided notable liver protection, reducing glucose (93.2mg/dl), ALT (42.3U/l), and AST (105.0U/l) levels, thus restoring liver health.

Table 4: Effect of dietary doses of SeNPs on haematology parameters of yellow grub-infected Nile tilapia.

Treatments	Control	T1	T2	T3	T4	T5	T6	T7
RBCs $\times 10^6/\mu\text{l}$	1.46c	1.95b	2.0ab	2.3a	2.1ab	1.2d	2.1ab	2.0ab
PCV %	25.9cd	27.2c	27.9b	28.2b	27.5cd	22.5e	26.3cd	25.1d
MCV (fl)	182ab	162c	166c	172b	169c	189a	170b	168c
MCHC (g/dl)	24.3c	31.0b	31.9b	33.5a	32.5ab	22.9c	32.1ab	31.3b
Hb (g/dl)	6.11c	9.5ab	9.8a	9.9a	9.6ab	6.1c	9.1ab	9.0b
TLC $\times 10^3/\mu\text{l}$	31.5b	32.2b	26.2cd	24.3d	28.2c	39.7a	23.6d	22.3d
Heterophils $\times 10^3/\mu\text{l}$	8.4b	7.7b	7.4b	6.5c	7.3bc	10.5a	6.3c	6.0c
Lymphocytes $\times 10^3/\mu\text{l}$	22.8b	20.89b	17.2cd	14.5e	16.6d	26.2a	18.3c	20.99b
Eosinophils $\times 10^3/\mu\text{l}$	0.0b	0.0b	0.0b	0.0b	0.0b	0.9a	0.0b	0.0b
Monocytes $\times 10^3/\mu\text{l}$	0.88b	0.79bc	0.75c	0.67d	0.72c	1.3a	0.69cd	0.75c

Note: Red blood cells (RBCs), packed cell volume (PCV), mean corpuscular volume (MCV), mean cell hemoglobin concentration (MCHC), hemoglobin (Hb), Total Leukocyte Count (TLC), The first group was control, T1, T2, and T3 were Nile tilapia fish treated with selenium nanoparticles (50, 100, and 200 mg/kg), T4 was praziquantel-treated fish, T5 was yellow grub infected fish, T6 was yellow grub infected and treated with Selenium nanoparticles at 200 $\mu\text{g}/\text{kg}$, while T7 was yellow grub infected fish and treated with the antiparasitic drug (200 $\mu\text{g}/\text{kg}$). Different lowercase letters indicate significant differences in the same raw data at $P < 0.05$.

Immune responses were severely suppressed in infected, untreated fish, as indicated by the lowest NBT (0.21), lysozyme (1.00 $\mu\text{g}/\text{mL}$), immunoglobulin (15.0 $\mu\text{g}/\text{mL}$), and total protein (34.0mg/dL). SeNPs at increasing doses improved these parameters, with T3 surpassing even the control levels in immune stimulation (NBT: 0.88, lysozyme: 1.82 $\mu\text{g}/\text{mL}$, immunoglobulin: 32.0 $\mu\text{g}/\text{mL}$, total protein: 65.0mg/dL).

Table 5: Serum Biochemical Parameters, Immune Activity, and Hormone Levels of Nile Tilapia (*Oreochromis niloticus*) Infected with Yellow Grub and Treated with Selenium Nanoparticles (SeNPs) and Praziquantel

Treatments	SeNPs ($\mu\text{g}/\text{kg}$ diet)	Antiparasitic agent	Liver function			Innate immune response				Hormones			Cortisol GH ($\mu\text{g}/\text{mL}$)		
			Glucose (mg/dl)	ALT (U/l)	AST (U/l)	NBT (Abs)	LYZ ($\mu\text{g}/\text{mL}$)	Ig ($\mu\text{g}/\text{mL}$)	TP (mg/dl)	FSH (nIU/mL)	T (ng/mL)	P4 (ng/mL)			
									M	F	XX				
Control	--	--	104.00d	56.00c	129.00b	0.42e	1.32e	23.00c	45.00cd	0.32d	0.98a	2.41e	0.92a	0.52e	3.66c
T1	50	--	98.33e	47.00d	121.00c	0.64c	1.55c	27.00b	60.55bc	0.48b	0.47d	2.85b	0.51b	0.69c	2.56e
T2	100	--	95.20f	44.00e	114.00d	0.68b	1.71b	31.00ab	62.40b	0.51ab	0.44de	2.92b	0.45c	0.75b	2.33f
T3	200	--	93.20f	42.30e	105.00e	0.88a	1.82a	32.00a	65.00a	0.57a	0.40e	3.15a	0.41d	0.88a	1.90h
T4	--	200	98.00e	47.35d	120.00d	0.65b	1.55c	28.30b	55.40c	0.50ab	0.51cd	2.82c	0.48c	0.78b	2.30g
T5	--	--	127.00a	83.00a	153.00a	0.21g	1.00g	15.00d	34.00e	0.21e	0.82b	2.11	0.56b	0.48d	5.89a
T6	200	--	103.00d	46.00d	122.00c	0.52d	1.36e	23.00c	50.00c	0.45c	0.51cd	2.68c	0.48c	0.62c	2.42d
T7	--	200	107.00c	52.00c	134.00b	0.50d	1.45d	26.60b	54.00c	0.48b	0.59c	2.75c	0.43d	0.59d	2.55d

ALT, Alanine transaminase; AST, Aspartate transaminase; NBT, Nitrobluetetrazolium; LYZ, lysozyme; TP, Total protein; M, Male; F, Female; T, Testosterone; P4, Progesterone; GH, Growth hormone. Means in the same column with lowercase different letters are significantly different at $P \leq 0.05$.

Hormonal disturbances were evident with infection: male FSH and female testosterone levels were lowest in T5 and best restored in T3, which also showed the highest progesterone levels (3.15 ng/mL) and growth hormone levels (0.88 ng/mL). Cortisol, a stress marker, was highest in T5 (5.89 µg/mL), but treatment with T3 reduced it to 1.90 µg/mL, indicating strong anti-stress effects.

Praziquantel (T4) offered moderate improvements but was less effective than high-dose SeNPs. Other groups receiving lower-dose SeNPs or remaining untreated showed only partial recovery. Statistical analysis confirmed that SeNPs at 200 µg/kg were the most effective intervention for restoring health, boosting immunity, balancing hormones, and reducing stress in infected tilapia.

The effect of SeNPs on the fold change in gene expression of infected fish: Gene expression analysis in Fig. 5 illustrates the significant impact of selenium nanoparticles (SeNPs) on growth and muscle gene regulation in Nile tilapia, particularly under yellow grub infection. Growth hormone receptor (GHR) expression increases significantly with T3 SeNPs (200mg/kg, approximately 7-fold), followed by T6 (~6-fold) and T4 (~5-fold), whereas infected, untreated fish (T5) exhibit substantial suppression (~1-fold). SeNPs notably restore GHR in infected fish, supporting their role in growth recovery. Myostatin (MSTN), typically a muscle growth inhibitor, is highest in the T3 and T4 groups (~28-fold and ~20-fold), but remains low in the T5 group (~2-fold), indicating infection-related metabolic impairment. T6 and T7 show moderate MSTN recovery (~15–16-fold).

Myogenin (MYOG) and myogenic Factor 6 (MYF6) expression is highest at T3, reflecting boosted muscle differentiation (~3.5-fold for MYOG, ~2-fold for MYF6), but is strongly suppressed by infection in T5. Treated infected groups (T6, T7) partially recover, with T6 exhibiting a more pronounced MYOG response (~2.5-fold). For elongation factor (ef1a), T3 and T4 peak (~5.5–6-fold), T5 is low (~1-fold), and T6 also shows robust recovery (~4-fold).

Histological study on the gills of yellow grub-infected Nile tilapia fish: Fig. 6 shows a comparison of gill histology, revealing distinct pathological patterns across treatment groups, which highlights the protective effects of selenium nanoparticles against yellow grub-induced gill damage in Nile tilapia. Control and SeNP-treated groups (Fig. 6A-D) demonstrate well-preserved gill architecture with intact primary lamellae and regularly arranged secondary lamellae. The respiratory epithelium appears intact with normal lamellar spacing and cellular organization. Fig. 6E (T4 - Praziquantel) similarly shows normal gill morphology, indicating that praziquantel treatment alone does not cause gill tissue damage. Fig. 6F shows that T5 (yellow grub-infected fish) exhibits dramatic gill pathology consistent with *Clinostomum* infection effects documented in the literature. The histology reveals inflammation and fusion of secondary lamellae, swollen tips (club-shaped), and multifocal basophilic spots of necrotic cells. The arrows in Fig. 6F point to areas of severe lamellar fusion, epithelial hyperplasia, and inflammatory cell infiltration. Additionally, T6 (infected + 200 µg/kg SeNPs, Fig. 6G) exhibits a remarkable histological

improvement compared to the infected control (Fig. 5F). While some residual pathological changes remain, there is clear evidence of tissue repair with reduced lamellar fusion and improved epithelial integrity. In T7 (infected + antiparasitic drug, Fig. 6H), a moderate histological improvement is demonstrated, but the recovery is less pronounced compared to SeNP treatment (Fig. 6G). Some lamellar fusion and inflammatory changes persist, suggesting that conventional antiparasitic therapy alone may be insufficient for complete restoration of the gill tissue in yellow grub infections.

The superior protective effects of SeNPs (Fig. 6G) compared to conventional antiparasitic treatment (Fig. 6H) suggest that selenium nanoparticles provide multifaceted benefits, including antioxidant protection, anti-inflammatory effects, and enhanced tissue repair mechanisms. The dose-dependent protective effects observed in uninfected SeNPs groups (Fig. 6B-D) indicate that prophylactic SeNP supplementation could prevent or minimize gill damage in *Clinostomum*-endemic environments.

Bacterial count in the water of yellow grub-infected fish: Table 6 shows that selenium nanoparticles (SeNPs) have superior antimicrobial effects compared to the antiparasitic agent. Treatments T2 (100 µg/Kg) and T3 (200 µg/Kg) consistently had the lowest bacterial counts, reducing total bacteria and *Aeromonas* by 1.5 to 2.0 log CFU/mL compared to controls. The antimicrobial effect of SeNPs is dose-dependent, with T1 (50 µg/Kg) showing moderate efficacy. Interestingly, T6 (200 µg/Kg) was slightly less effective than T3, possibly due to experimental differences. The antiparasitic agent (T4, T7) had moderate activity but was less effective than SeNPs. While all groups displayed bacterial growth over time, the SeNP-treated groups experienced slower increases, with T3 showing the most stable suppression throughout the 10 weeks.

Bacterial count in the organs of yellow grub-infected fish: The data in Table 7 demonstrate statistically significant reductions in both total bacterial and total *Aeromonas* counts in fish organs following dietary supplementation with SeNPs, especially at increasing doses (T1–T3), compared to the control and other treatments. Across all tissue types—skin, muscle, intestine, and gills—the groups receiving SeNPs (particularly T2 and T3: 100 and 200 µg/kg diet) consistently show significantly lower means (indicated by non-overlapping lowercase letters) relative to the control. The T3 group exhibited the lowest total bacterial counts across all organs (e.g., skin: 5.1e, muscle: 3.3e), and the lowest *Aeromonas* counts (e.g., skin: 3.1d, muscle: 2.1d, intestine: 2.7d, gills: 3.1d), with all values differing significantly from the control group (e.g., skin: 4.3ab, muscle: 3.2ab, intestine: 4.2ab, gills: 4.6b for *Aeromonas*). The significant decline in both general and *Aeromonas*-specific bacterial loads indicates that SeNPs, particularly at higher doses, are effective at reducing overall bacterial colonization and targeted pathogen burden in Tilapia tissues. In contrast, the antiparasitic agent group (T4 and T7) and the combined treatment (T6) showed moderate decreases in bacterial and *Aeromonas* counts; however, these reductions were generally less pronounced than those observed in the high-dose SeNPs group. The group with no intervention (T5) had the highest counts, further supporting the antimicrobial role of SeNPs.

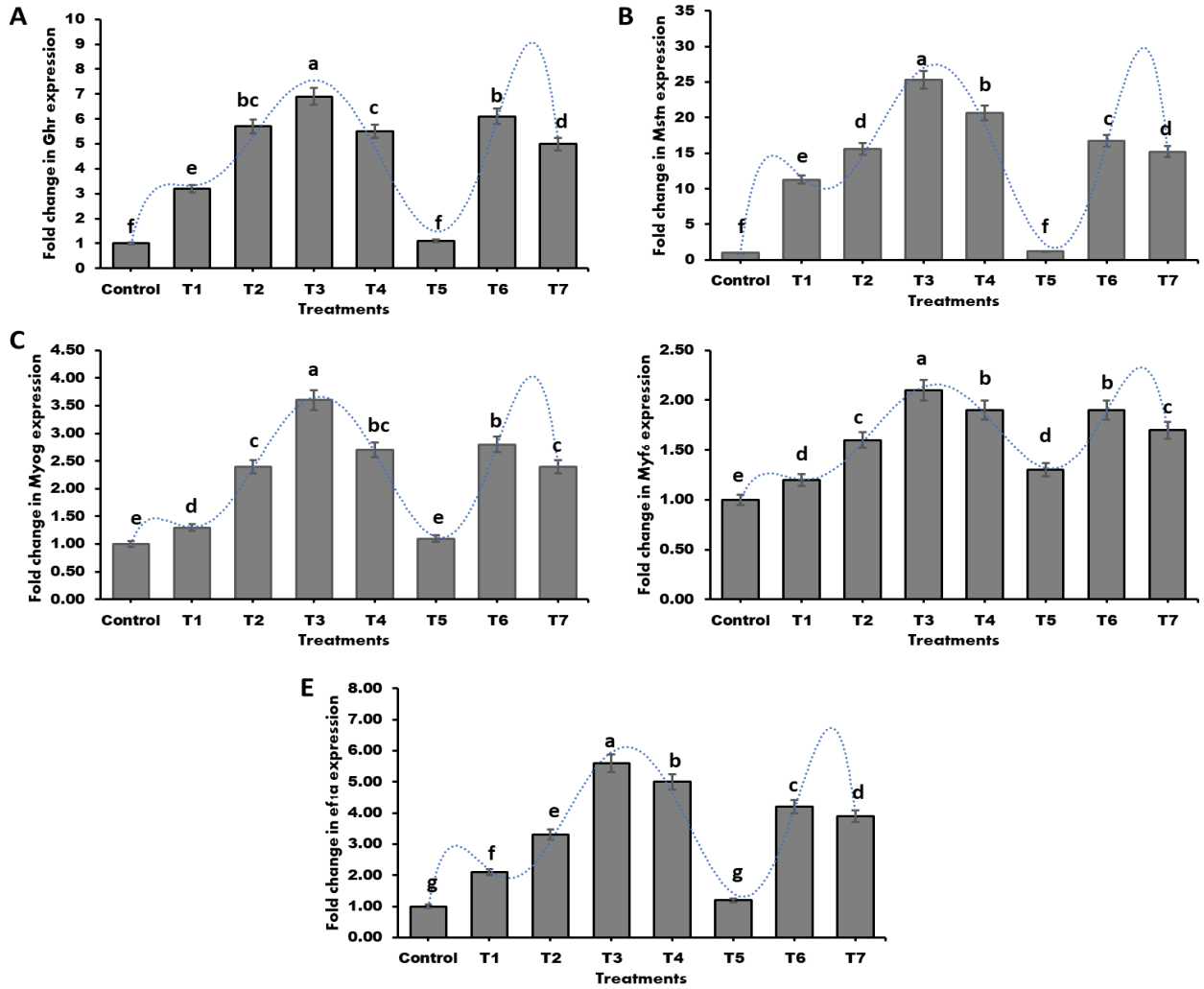


Fig. 5: The effect of SeNPs on the fold change in gene expression of (A) *ghr*, (B) *mstn*, (C) *myog*, (D) *myf6*, and (E) *eflα* in yellow grub-infected Nile tilapia fish. the first group was control, T1, T2, and T3 were Nile talipa fish treated with selenium nanoparticles (50, 100, and 200 mg/kg), T4 was praziquantel-treated fish, T5 was yellow grub infected fish, T6 was yellow grub infected and treated with Selenium nanoparticles at 200 µg/kg, while T7 was yellow grub infected fish and treated with the antiparasitic drug (200 µg/kg).

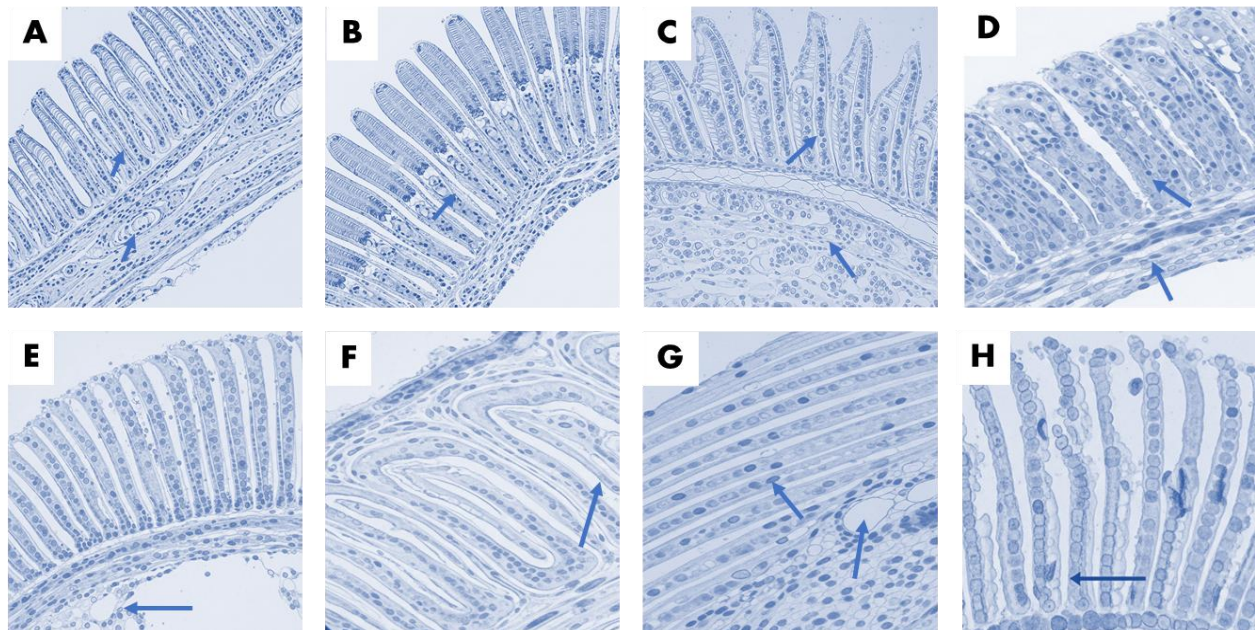


Fig. 6: The gills of yellow grub-infected Nile Tilapia fish and treated with selenium nanoparticles (SeNPs) and Praziquantel, where the first group was control, T1, T2, and T3 were Nile Talipa fish treated with selenium nanoparticles (50, 100, and 200 mg/kg), T4 was praziquantel-treated fish, T5 was yellow grub infected fish, T6 was yellow grub infected and treated with Selenium nanoparticles at 200 µg/kg, while T7 was yellow grub infected fish and treated with the antiparasitic drug (200 µg/kg).

Table 6: The total bacterial count (Log CFU/mL) and total *Aeromonas* count (Log CFU/mL) in water during the 10 experimental period

Treatments	SeNPs (µg/kg) diet	Antiparasitic agent	Total bacterial count CFU/mL				Total <i>Aeromonas</i> count CFU/mL			
			Experimental period (week)							
			1	4	8	10	1	4	8	10
Control	--	--	5.5a	5.8a	5.9a	6.2a	2.8a	3.2a	3.7a	4.2a
T1	50	--	4.1bc	4.4c	4.7d	5.0c	2.1c	2.5c	2.8c	3.1c
T2	100	--	3.6cd	3.8c	4.2d	4.5d	1.9d	2.2d	2.5d	2.7d
T3	200	--	3.3d	3.5d	4.0d	4.2d	1.5d	1.8d	2.1d	2.4d
T4	--	200	3.6cd	3.8d	4.3d	4.5d	1.8d	2.0d	2.3d	2.6d
T5	--	--	5.8a	6.0a	6.3ab	6.6ab	2.6ab	2.8ab	3.2ab	3.5ab
T6	200	--	3.8c	4.0c	4.4d	4.7c	2.0c	2.4c	2.7c	2.9d
T7	--	200	4.4b	4.7b	4.9c	5.2b	2.4c	2.6c	2.9c	3.1c

Means in the same column with lowercase different letters are significantly different at $P \leq 0.05$.

Table 7: The total bacterial count and total *Aeromonas* count in *Talipa* fish organs expressed as (Log CFU/g) after 10 weeks

Treatments	SeNPs (µg/kg) diet	Antiparasitic agent	Total bacterial count				Total <i>Aeromonas</i> spp.			
			Fish organs							
			Skin	Muscle	Intestine	Gills	Skin	Muscle	Intestine	Gills
Control	--	--	7.2ab	5.8ab	7.4ab	7.9b	4.3ab	3.2ab	4.2ab	4.6b
T1	50	--	5.9d	4.2d	6.1d	6.7c	3.6c	2.4b	3.4c	3.8c
T2	100	--	5.5de	3.8e	5.5e	6.1e	3.4c	2.2c	3.1d	3.4d
T3	200	--	5.1e	3.3e	5.2e	5.6e	3.1d	2.1d	2.7d	3.1d
T4	--	200	5.7d	4.1d	5.9e	6.2e	3.6c	1.9d	3.1d	3.4d
T5	--	--	7.6a	5.8a	8.0a	8.3a	4.4a	3.3a	4.6a	5.2a
T6	200	--	6.0c	4.2d	6.2d	6.4d	3.6c	2.4c	3.6c	3.8c
T7	--	200	6.3c	4.6c	6.6c	6.9c	4.1b	2.8b	3.6c	3.8c

Means in the same column with different lowercase letters are significantly different at $P \leq 0.05$.

DISCUSSION

The presence of yellow grub (metacercariae of digenaeans trematodes) can significantly impact the health and marketability of Nile tilapia (Ahmed, 2024). These parasites commonly infest fish, leading to visible lesions, reduced growth rates, and compromised immune function (Di Cesare *et al.*, 2024). Heavy infestations can cause physical damage to tissues and organs, making fish more susceptible to secondary bacterial or fungal infections (Islam *et al.*, 2024). Studies by Abd-ELrahman *et al.* (2023) have extensively documented the pathological effects of digenaeans trematodes on fish, including reduced fitness and susceptibility to other diseases. Beyond the direct physiological harm, the visible cysts of yellow grub detract from the fish's aesthetic appeal, leading to economic losses for aquaculture producers due to reduced market value and consumer rejection, as highlighted by Mahdy *et al.* (2024a). This highlights the crucial need for effective strategies to mitigate parasitic burdens in farmed tilapia populations.

Selenium (SeNPs) and antiparasitic agents offer promising avenues for managing yellow grub infestations and alleviating their adverse effects on Nile tilapia (Mahdy *et al.*, 2024b). Selenium, particularly in its nano form (SeNPs), has been recognized for its potent antioxidant and immunomodulatory properties (Vijayaram *et al.*, 2025). By bolstering the fish's immune system, selenium can enhance its natural resistance to parasitic infections (Eissa *et al.*, 2024). This may involve improved cellular immunity, increased production of protective antibodies, or enhanced inflammatory responses (Saad *et al.*, 2022), which help encapsulate or eliminate parasites. For instance, Eissa *et al.* (2024) demonstrated that selenium supplementation can improve immune responses in fish challenged with parasites. Furthermore, selenium's role in reducing oxidative stress can help counteract the tissue damage caused by parasitic invasion, thereby promoting overall fish health and recovery, a mechanism supported by Yazhiniprabha *et al.* (2022).

Antiparasitic agents, such as Praziquantel, on the other hand, directly target the parasites, aiming to reduce or eliminate their presence within the fish (Rigos *et al.*, 2024). These agents can work through various mechanisms, such as disrupting the parasite's nervous system, inhibiting its metabolic pathways, or damaging its structural integrity. Research by Garbin *et al.* (2024) and Reda *et al.* (2024) has explored the efficacy of various antiparasitic compounds in controlling parasitic infections in aquaculture. The judicious use of effective antiparasitic compounds, in conjunction with improved husbandry practices, is vital for controlling parasitic loads in aquaculture systems. Combining the immune-boosting effects of selenium with the direct action of antiparasitic agents could offer a multi-pronged approach to effectively mitigate the adverse impacts of yellow grub on Nile tilapia, leading to healthier fish and more sustainable aquaculture production.

The key mechanisms through which SeNPs exert their beneficial effects against parasitic infections, which often induce significant oxidative stress in the host (Pawłowska *et al.*, 2023). This occurs as the host's immune system mounts a response (e.g., producing reactive oxygen species, or ROS) and also as a result of the parasitic metabolic activities. SeNPs are renowned for their strong antioxidant properties (Sentkowska and Pyrzyńska, 2023). They can directly scavenge free radicals and, more importantly, act as precursors for synthesizing crucial selenoenzymes, such as glutathione peroxidase (GPx), thioredoxin reductase (TrxR), and catalase (CAT) (Song *et al.*, 2022). These enzymes are vital components of the host's endogenous antioxidant defense system (Ponnampalam *et al.*, 2022). By enhancing these antioxidant defenses, SeNPs help to neutralize harmful ROS, reduce lipid peroxidation, prevent cellular damage, and maintain the integrity of host tissues (e.g., intestinal epithelium, blood cells) that the parasitic infection might otherwise compromise. This protective effect enables the host to cope more effectively with the stress of infection and recover more quickly.

Selenium is an essential micronutrient for a properly functioning immune system (Lungu *et al.*, 2022). SeNPs can significantly modulate both innate and adaptive immune responses (Chen *et al.*, 2022). They can enhance the activity of various immune cells, including macrophages, lymphocytes (T-cells and B-cells), and natural killer (NK) cells. A stronger immune response enables the host to recognize parasites more effectively, encapsulate them, and potentially eliminate or control their parasitic stages. SeNPs can influence the production of cytokines, promoting a balanced immune response that is effective against the parasite without causing excessive inflammation and collateral tissue damage to the host (Liu *et al.*, 2024). They can help reduce pro-inflammatory cytokines that might be elevated during parasitic infections (Khabatova *et al.*, 2022). By boosting overall immune competence, SeNPs increase the host's resistance to infection and reduce its susceptibility to secondary infections that often accompany parasitic burdens.

Beyond direct immune enhancement, the antioxidant and anti-inflammatory properties of SeNPs directly contribute to protecting host tissues and organs from parasitic damage (Abdel-Gaber *et al.*, 2023). For yellow grub, which encysts in fish tissues, SeNPs can help reduce the inflammatory reactions around the cysts, minimize tissue damage, and potentially aid in the encapsulation or isolation of the parasite, limiting its pathological impact. Studies have shown that SeNPs ameliorate hepatic histopathology, reduce granuloma diameters, and improve intestinal integrity in hosts infected with various parasites (Alabbassy *et al.*, 2024).

In summary, selenium nanoparticles do not directly kill yellow grub. The antiparasitic mechanism is largely host-mediated, involving a synergistic action that reduces oxidative stress caused by the infection (Chen *et al.*, 2022). Enhancing the host's immune response, thereby increasing its capacity to resist and cope with the parasite (Mi *et al.*, 2022). Protecting host tissues from inflammation and damage induced by the parasitic presence. This makes them a valuable *supportive* agent in managing parasitic diseases, particularly in aquaculture, by improving fish health and resilience.

The current study builds on existing research, revealing that dietary supplementation with 200 µg SeNPs per kg of diet significantly enhanced the growth performance of Nile tilapia. This finding aligns with previous studies that also documented positive growth effects at the same SeNP dosage (Ghaniem *et al.*, 2022). This observed improvement in growth can be attributed to several factors. SeNPs likely increase intestinal absorption and improve bioavailability (Lee *et al.*, 2016), resulting in more selenium being effectively utilized by the fish. Selenium is crucial for synthesizing selenoproteins, which contribute to higher protein levels in the intestinal villi, subsequently improving digestive enzyme activity, feed efficiency, metabolism, and overall growth (Mehdi *et al.*, 2013). Additionally, selenium enhances the intestinal microbial population and activity, as well as protease activity, resulting in improved protein utilization and digestibility. Ibrahim *et al.* (2021b) further linked SeNP-induced growth promotion to an increase in the mucosal length and width of the intestinal epithelium, thereby expanding the surface area for nutrient absorption.

The treatment groups in our experiment demonstrated an impressive 25% improvement in Feed Conversion Ratio (FCR) compared to the control fish, a result consistent with that of Abu-Elala *et al.* (2021). FCR is a critical metric in aquaculture, directly reflecting how efficiently fish convert feed into biomass. Given that feed costs represent over half of the variable operating costs in aquaculture (Dunham and Elasad, 2018), the substantial FCR improvement observed with SeNP supplementation highlights its significant economic benefits for tilapia farming. Furthermore, the present results indicate that dietary SeNPs at 1.0 mg/kg also increased survival time and decreased mortality rates, aligning with the findings of Sheikh *et al.* (2024).

Blood parameters serve as valuable indicators of an animal's overall health. These findings are consistent with previous research on Nile tilapia fed a similar SeNP dosage (1.0 mg/kg) (Abu-Elala *et al.*, 2021; Rathore *et al.*, 2023). Higher RBC counts, HCT, Mean Corpuscular Volume (MCV), and Mean Corpuscular Hemoglobin (MCH) were also observed in genetically improved farmed tilapia (GIFT) fed 0.75 mg/kg SeNPs (Joshna *et al.*, 2023). Moreover, Ibrahim *et al.* (2021b) noted that Nile tilapia fed dietary SeNPs (0.8 mg/kg) had superior HCT, Hb, RBCs, and WBCs compared to those fed bulk selenium or control diets. These findings suggest that SeNPs regulate metabolic rate, as a higher number of RBCs and Hb content correlates with greater oxygen availability in body tissues (Parrino *et al.*, 2018). The antioxidant properties of selenium play a crucial role in this process, protecting RBCs and extending their lifespan by guarding against reactive oxygen species (ROS), thereby preventing membrane disruption, cell hemolysis, and degeneration, and maintaining erythrocyte health and integrity (Ashouri *et al.*, 2015).

The current study found that treated fish, particularly those at T5, exhibited the highest levels of AST and ALT, which is consistent with the findings of Radwan *et al.* (2021). Notably, the study revealed significantly higher total serum protein, albumin, and globulin levels in the two SeNP treatment groups, with even higher levels in T3 and T6 compared to the control fish. Similar observations have been documented in the Nile tilapia (Rathore *et al.*, 2021; Eissa *et al.*, 2024) specifically reporting higher serum globulin levels in Nile tilapia fed SeNPs. Importantly, the current findings revealed no significant difference in glucose levels between the experimental groups, suggesting that selenium may have potential in alleviating stress and optimizing the physiological conditions of fish (Kumar *et al.*, 2020).

In teleost fish, a positive correlation exists between growth rate and hepatic *ghr-1* mRNA levels (Ruan RuiXia *et al.*, 2011), supporting the use of the *ghr* gene as a growth indicator. Our results showed that SeNP supplementation in T3 and T6 increased *ghr* expression by an impressive 5.038-fold and by 1.65-fold in T1, compared to the control fish. Fasil *et al.* (2021) similarly found that SeNPs increased *gh* expression in zebrafish muscle, and Abd El-Kader *et al.* (2020) reported *gh* upregulation in European sea bass fed a SeNP diet. Variations in *ghr* expression across different tissues and fish species (Otero-Tarrazón *et al.*, 2023) may be attributed to the unique characteristics of nano-form minerals.

Fish skeletal muscle grows post-embryonically through hypertrophy or hyperplasia, driven by the activity of undifferentiated myosatellite cells (Rbbani *et al.*, 2024). Myogenin (*myog*) plays a crucial role in myogenesis, regulating muscle cell differentiation and satellite cell growth (Girolamo *et al.*, 2024). Activated satellite cells differentiate and divide to produce new muscle fibers (Ralli re *et al.*, 2023), contributing to both muscle hyperplasia and hypertrophy. Myogenin is also essential for myocyte fusion, which increases nuclear number and subsequently leads to the typical development of fiber size, while restricting the size of the myonuclear domain in juvenile and adult muscles (Ortuste Quiroga *et al.*, 2022). Our study showed a 1.248-fold increase in *myog* expression in the T3 and T6 groups compared to the control or T1 groups. This finding aligns with Gao *et al.* (2018), who reported that selenium increased satellite cell proliferation and incorporation into muscle fiber cells, as well as the expression of MyoD and MyoG.

Conversely, MYF6 regulates the expression of muscle-specific genes, controlling myogenesis and muscle regeneration (Wang *et al.*, 2022). Moretti *et al.* (2016) reported that MYF6 negatively regulates adult skeletal muscles, as evidenced by increased muscle fiber size after *myf6* gene knockdown. The observed higher expression of muscle-specific genes and increased protein synthesis further explain the increase in muscle fiber. Zou *et al.* (2015) identified single-nucleotide polymorphisms (SeNPs) within *myf6* in Nile tilapia that were positively associated with body weight, depth, and length. In our research, *myf6* expression levels decreased in T1, T3, and T6 compared to the control group, suggesting a beneficial effect on muscle growth.

In our study, myostatin (*mstn*) expression increased by 20.66-fold in T3 and T6 and 11.5-fold in T1 compared with infected fish. This finding contrasts with that of Ibrahim *et al.* (2021a), who suggested that *mstn* expression decreased in Nile tilapia when given selenium-loaded chitosan nanoparticles. These discrepancies might stem from differences in developmental stage, muscle type, and nutritional state (Patruno *et al.*, 2008), all of which can influence *mstn* regulatory mechanisms. Elevated blood cortisol levels have also been correlated with higher *mstn* expression in fish (ELbially *et al.*, 2023), which could potentially explain the increased *mstn* expression in T3 and T6 due to higher cholesterol levels.

Myostatin (MSTN) is a member of the transforming growth factor β superfamily, which negatively regulates the proliferation and differentiation of skeletal muscle cells, thereby limiting their growth (Sun *et al.*, 2012). Possible changes in this gene (e.g. point mutations/SNP) lead to an increase in skeletal muscle mass (McPherron *et al.*, 1997). In sharp contrast to mammals, MSTN orthologs of various fish species are widely expressed with a tissue-specific expression pattern. In mammals, it is primarily expressed in skeletal muscle, at lower levels in adipose tissue, the mammary gland, and cardiac muscle. In fish, MSTN mRNA has also been detected in other tissues/organs (brain, eye, intestine, gill fibers, gonad, kidney) (Maccatrozzo *et al.*, 2001). Two distinct myostatin genes have also been found in some fish species (Roberts and Goetz, 2001). Comparison of myostatin sequences revealed that myostatin was extremely well conserved during

evolution, to the extent that in bony fish, such as salmonoids, additional copies of the MSTN gene could be retained due to duplication of the ancient genome (Gabillard *et al.*, 2013). Some of the potential SNPs in MSTN may have a positive effect on growth properties: for example, Fish MSTN, on the other hand, is responsible for cell proliferation and overall inhibition of cell growth, so although it regulates tissue mass, it does not specialize as a potent muscle regulator (Gabillard *et al.*, 2013). In contrast to mammalian muscle growth, where postnatal muscle growth occurs almost exclusively with hypertrophy, in most fish species, postnatal muscle growth is a combination of hyperplasia and hypertrophy (Galt *et al.*, 2014).

The results strongly indicate that SeNPs promote muscle fiber hypertrophy, thereby enhancing the growth rate. In rainbow trout, selenium has been shown to induce hypertrophic muscle growth by enhancing selenoprotein gene expression (specifically SelK and SelW), inhibiting protein breakdown via the ubiquitin-proteasome pathway and the calpain system, and promoting myoblast fusion into pre-existing muscle fibers (Wang *et al.*, 2021).

Conclusions: This study highlights the significant potential of biosynthesized selenium nanoparticles (SeNPs) as a sustainable and multifunctional solution for managing *Clinostomum marginatum* infections in Nile tilapia aquaculture. By leveraging the eco-friendly synthesis of SeNPs using *Saccharomyces cerevisiae*, we present a viable alternative to conventional chemical antiparasitic agents, which are often associated with environmental concerns, drug resistance, and residual toxicity. The unique properties of SeNPs—including their antioxidant, antibacterial, and immunomodulatory capabilities—position them as a comprehensive therapeutic agent capable of addressing not only parasitic infections but also secondary bacterial challenges and oxidative stress in farmed fish. Beyond disease control, SeNPs demonstrate remarkable potential in enhancing growth performance and physiological resilience, making them a valuable tool for improving overall aquaculture productivity. The findings underscore the importance of nanotechnology in advancing sustainable aquaculture practices, offering a paradigm shift toward environmentally friendly disease management. Future research should focus on optimizing dosage protocols, evaluating long-term safety, and exploring large-scale applications to realize the commercial potential of SeNPs in aquaculture. By integrating SeNPs into current aquaculture systems, stakeholders can achieve improved fish health, reduced reliance on chemical treatments, and enhanced production efficiency, ultimately contributing to global food security and sustainable aquatic farming practices.

Competing interests: The authors declare that they have no competing interests.

Author Contributions: Conceptualization, HHA, MNA, HASR, MAA, and AM, formal analysis, AAA, HAM, HA, MS, SHA, and AEA, investigation, HHA, MNA, HASR, MAA, and AM, data curation, AAA, HAM, HA, MS, SHA, and AEA, writing original draft preparation, HHA, MNA, HASR, MAA, and AM, writing final manuscript and

editing, AAA, HAM, HA, MS, SHA, and AEA, visualization and methodology, HHA, MNA, HASR, MAA, AM, AAA, HAM, HA, MS, SHA, and AEA. All authors have read and agreed to the published version of the manuscript.

Acknowledgements: The authors gratefully acknowledge Princess Nourah bint Abdulrahman University Researchers Supporting Project number (PNURSP2025R460), Princess Nourah bint Abdulrahman University, Riyadh, Saudi Arabia. The authors extend their appreciation to the Deanship of Research and Graduate Studies at King Khalid University for funding this work through Large Research Project under grant number RGP2/330/46.

Funding: This research was funded by Princess Nourah bint Abdulrahman University Researchers Supporting Project number (PNURSP2025R460), Princess Nourah bint Abdulrahman University, Riyadh, Saudi Arabia. King Khalid University for funding this work through Large Research Project under grant number RGP2/330/46.

REFERENCES

- Abd-Elrahman SM, Gareh A, Mohamed HI, et al., 2023. Prevalence and morphological investigation of parasitic infection in freshwater fish (*Nile tilapia*) from upper Egypt. *Animals* 13(6): 1088.
- Abd El-Kader MF, El-Bab AFF, Shoukry M, et al., 2020. Evaluating the possible feeding strategies of selenium nanoparticles on the growth rate and wellbeing of European seabass (*Dicentrarchus labrax*). *Aquac Rep* 18:100539.
- Abdel-Gaber R, Hawsah MA, Al-Otaibi T, et al., 2023. Biosynthesized selenium nanoparticles to rescue coccidiosis-mediated oxidative stress, apoptosis and inflammation in the jejunum of mice. *Front Immunol* 14:1139899.
- Abduljabbara BT, El-Zayat MM, El-Halawany E-SF, et al., 2024. Selenium nanoparticles from *Euphorbia retusa* extract and its biological applications: antioxidant, and antimicrobial activities. *Egypt J Chem* 67:463-472.
- Abu-Elala NM, Shaalan M, Ali SE, et al., 2021. Immune responses and protective efficacy of diet supplementation with selenium nanoparticles against cadmium toxicity in *Oreochromis niloticus*. *Aquac Rep* 52:3677-3686.
- Ahmad N, Hussain S, Azam S, et al., 2022. Effects of Se nanoparticles supplementation on growth performance, hematological parameters and nutrient digestibility of *Labeo rohita* fingerling fed sunflower meal-based diet. *Braz J Biol* 84:e253555.
- Ahmed O. 2024. Control measure of fishborne zoonotic trematodes: A Review. *Aquatic Science and Fish Resources (ASFR)* 5:76-84.
- Al-Deriny SH, Dawood MA, Abou Zaid AA, et al., 2020. The synergistic effects of *Spirulina platensis* and *Bacillus amyloliquefaciens* on the growth performance, intestinal histomorphology, and immune response of Nile tilapia (*Oreochromis niloticus*). *Aquac Rep* 17:100390.
- Al-Wakeel AH, Elbahnasy S, El-Moaty AA, et al., 2024. Green synthesis and characterization of SeNPs using *Pediastrum boryanum* extract and evaluation of their biological activities. *Mansoura Vet Med J* 25 (1) 1-19.
- Alabbassy MM, Ismail OA, Elskeikh IA, 2024. Effectiveness of selenium nanoparticles in treatment of schistosoma mansoni infected mice. *J Egypt Soc Parasitol* 54:259-266.
- Alqaraleh SY, Al-Zereini WA, Mwafi NR, et al., 2024. The green synthesis of selenium nanoparticles: a comprehensive review on methodology, characterization and biomedical applications. *Res J Pharm Technol* 17:4054-4062.
- Alsulami MN, El-Saadony MT, 2023. Supplementing broiler diets with bacterial selenium nanoparticles enhancing performance, carcass traits, blood indices, antioxidant status, and caecal microbiota of *Eimeria tenella*-infected broiler chickens. *Poult Sci* 102:103111.
- Alsulami MN and El-Saadony MT, 2024. The enhancing effect of bacterial zinc nanoparticles on performance, immune response, and microbial load of Nile Tilapia (*Oreochromis niloticus*) by reducing the infection by *Trichodina heterodontata*. *Pak Vet J* 44(3): 599-610.
- Ashouri S, Keyvanshokoh S, Salati AP, et al., 2015. Effects of different levels of dietary selenium nanoparticles on growth performance, muscle composition, blood biochemical profiles and antioxidant status of common carp (*Cyprinus carpio*). *Aquaculture* 446:25-29.
- Caneschi A, Bardhi A, Barbarossa A, et al., 2023. The use of antibiotics and antimicrobial resistance in veterinary medicine, a complex phenomenon: A narrative review. *Antibiotics* 12:487.
- Chen G, Yang F, Fan S, et al., 2022. Immunomodulatory roles of selenium nanoparticles: Novel arts for potential immunotherapy strategy development. *Front Immunol* 13:956181.
- Dacie JV and Lewis SM, 1980. Blood count. In: *Practical haematology*. In *Practical haematology* (6th ed. ed., pp. 24-55). London, Churchill.
- Garbin LE, Servián A, Fuentes L, et al., 2024. Phylogenetic relationship between *Contraecum* spp. (Nematoda, Anisakidae) parasitizing cormorants (Aves, Phalacrocoracidae) in Argentina. *Parasitol Res* 123(1), 61.
- Dawood MA, Metwally AE-S, El-Sharawy ME, et al., 2020. The influences of ferulic acid on the growth performance, haemato-immunological responses, and immune-related genes of Nile tilapia (*Oreochromis niloticus*) exposed to heat stress. *Aquaculture* 525:735320.
- de Freitas Oliveira JW, Torres TM, Moreno CJG, et al., 2021. Insights of antiparasitic activity of sodium diethyldithiocarbamate against different strains of *Trypanosoma cruzi*. *Sci Rep* 11:11200.
- Di Cesare L, Montes MM, Vargas MS, et al., 2024. Yellow grub diseases on two seasonal killifish (*Cyprinodontiformes*, *Rivulidae*): a histopathological study. *Parasitol Res* 123:395.
- Dunham RA, Elswad A, 2018. Catfish biology and farming. *Annu Rev Anim Biosci* 6:305-325.
- Eissa E-SH, Bazina WK, Abd El-Aziz YM, et al., 2024. Nano-selenium impacts on growth performance, digestive enzymes, antioxidant, immune resistance and histopathological scores of Nile tilapia, *Oreochromis niloticus* against *Aspergillus flavus* infection. *Aquac Int* 32:1587-1611.
- El-Saadony MT, Alagawany M, Patra AK, et al., 2021a. The functionality of probiotics in aquaculture: An overview. *Fish Shellfish Immunol* 117: 36-52.
- El-Saadony MT, Alkhatib FM, Alzahrani SO, et al., 2021b. Impact of mycogenic zinc nanoparticles on performance, behavior, immune response, and microbial load in *Oreochromis niloticus*. *Saudi J Biol Sci* 28:4592-4604.
- El-Sherbiny MM, Orif MI, El-Hefnawy ME, et al., 2023. Fabrication of bioactive nanocomposites from chitosan, cress mucilage, and selenium nanoparticles with powerful antibacterial and anticancerous actions. *Front Microbiol* 14:1210780.
- Elbially ZI, Atef E, Al-Hawary II, et al., 2023. Myostatin-mediated regulation of skeletal muscle damage post-acute *Aeromonas hydrophila* infection in Nile tilapia (*Oreochromis niloticus* L.). *Fish Physiol Biochem* 49:1-17.
- FAO. 2022. The State of World Fisheries and Aquaculture 2022. Food and Agriculture Organization of the United Nations.
- Faramarzi S, Anzabi Y, Jafarizadeh-Malmir H, 2020. Nanobiotechnology approach in intracellular selenium nanoparticle synthesis using *Saccharomyces cerevisiae*—fabrication and characterization. *Arch Microbiol* 202:1203-1209.
- Fasil DM, Hamdi H, Al-Barty A, et al., 2021. Selenium and zinc oxide multinutrient supplementation enhanced growth performance in zebra fish by modulating oxidative stress and growth-related gene expression. *Front Bioeng Biotechnol* 9:721717.
- Fitzsimmons K, 2021. Tilapia: The most important aquaculture species of the 21st century. In *Tilapia in Intensive Co-culture* (pp. 3-15). Wiley-Blackwell.
- Freire BM, Lange CN, Cavalcanti YT, et al., 2024. The dual effect of Selenium nanoparticles in rice seedlings: From increasing antioxidant activity to inducing oxidative stress. *Plant Stress* 11:100372.
- Gabillard J-C, Biga PR, Rescan P-Y, et al., 2013. Revisiting the paradigm of myostatin in vertebrates: insights from fishes. *Gen Comp Endocrinol* 194:45-54.
- Galt NJ, Froehlich JM, Remily EA, et al., 2014. The effects of exogenous cortisol on myostatin transcription in rainbow trout, *Oncorhynchus mykiss*. *Comp Biochem Physiol A Mol Integr Physiol* 175:57-63.
- Gao J, Nie W, Wang F, et al., 2018. Maternal selenium supplementation enhanced skeletal muscle development through increasing protein synthesis and SelW mRNA levels of their offspring. *Biol Trace Elem Res* 186:238-248.

- George D, Lakshmi S, Sharma A, et al., 2023. Nanotechnology: A novel tool for aquaculture feed development. In: Nanotechnological approaches to the advancement of innovations in aquaculture: Springer. p 67-88.
- Ghaniem S, Nassef E, Zaineldin AI, et al., 2022. A comparison of the beneficial effects of inorganic, organic, and elemental nano-selenium on Nile tilapia: growth, immunity, oxidative status, gut morphology, and immune gene expression. *Biol Trace Elem Res* 200:5226-5241.
- Girolamo DD, Benavente-Diaz M, Murolo M, et al., 2024. Extraocular muscle stem cells exhibit distinct cellular properties associated with non-muscle molecular signatures. *Development* 151: dev202144.
- Hu L, Ji X, Li J, et al., 2023. Selection of *Saccharomyces cerevisiae* isolates from helan mountain in China for wine production. *Fermentation* 9:376.
- Husseiny WA, Hassanin AA, El Nabtiti AA, et al., 2021. Silver nanoparticles as modulators of myogenesis-related gene expression in chicken embryos. *Genes* 12:629.
- Ibrahim D, Neamat-Allah AN, Ibrahim SM, et al., 2021a. Dual effect of Selenium loaded Chitosan Nanoparticles on growth, antioxidant, immune related genes expression, transcriptomics modulation of caspase 1, cytochrome P450 and heat shock protein and *Aeromonas hydrophila* resistance of Nile Tilapia (*Oreochromis niloticus*). *Fish shellfish Immunol* 110:91-99.
- Ibrahim MS, El-gendy GM, Ahmed AI, et al., 2021b. Nanoselenium versus bulk selenium as a dietary supplement: Effects on growth, feed efficiency, intestinal histology, haemato-biochemical and oxidative stress biomarkers in Nile tilapia (*Oreochromis niloticus* Linnaeus, 1758) fingerlings. *Aquac Res* 52:5642-5655.
- Ibrahim SSS, Ansari YN, Puri AV, et al., 2024. Recent progress in the green synthesis, characterization, and applications of selenium nanoparticles. *BIO Integration* 5:969.
- Ifijen IH, Atoe B, Ekun RO, et al., 2023. Treatments of *Mycobacterium tuberculosis* and *Toxoplasma gondii* with selenium nanoparticles. *BioNanoScience* 13:249-277.
- Islam SI, Rodkhum C, Taweethavonsawat P, 2024. An overview of parasitic co-infections in tilapia culture. *Aquac Int* 32:899-927.
- Joshna M, Ahilan B, Uma A, et al., 2023. Effect of selenium nanoparticles fortified diet on the growth performance, hematological responses, wholebody composition, intestinal microflora and histological alterations of GIFT. *Anim Nutr Feed Technol* 23:455-468.
- Khabatova VV, Serov DA, Tikhonova IV, et al., 2022. Selenium nanoparticles can influence the immune response due to interactions with antibodies and modulation of the physiological state of granulocytes. *Pharmaceutics* 14:2772.
- Khalil HS, Nasr-Allah A, 2025. Comparative study on the effect of raceway and In-Pond raceway systems on different Nile Tilapia, *Oreochromis niloticus* strains fed diets replacing soybean meal by poultry byproduct meal on: water quality, growth performance and production efficiency. *Aquac Int* 33:258.
- Khan Z, Thounaojam TC, Chowdhury D, et al., 2023. The role of selenium and nano selenium on physiological responses in plant: a review. *Plant Growth Regul* 100:409-433.
- Kumar N, Gupta SK, Chandan NK, et al., 2020. Mitigation potential of selenium nanoparticles and riboflavin against arsenic and elevated temperature stress in *Pangasianodon hypophthalmus*. *Sci Rep* 10:17883.
- Lee R, Foerster J, Jukens J, et al., 1998. Rodgers GM. *Wintrobe s-Clinical Hematology*. In: Lippincott Williams and Wilkins, New York, USA.
- Lee S, Nambi RVW, Won S, et al., 2016. Dietary selenium requirement and toxicity levels in juvenile Nile tilapia, *Oreochromis niloticus*. *Aquaculture* 464:153-158.
- Liu S, Li N, Lai H, et al., 2024. Selenium nanoparticles enhance NK cell-mediated tumoricidal activity in malignant pleural effusion via the TrxR1-IL-18RAP-pSTAT3 pathway. *Adv Funct Mater* 34:2401264.
- Livak KJ, Schmittgen TD, 2001. Analysis of relative gene expression data using real-time quantitative PCR and the 2⁻ΔΔCT method. *Methods* 25:402-408.
- Lungu I-I, Babarus I, Oniciuc L, et al., 2022. A review of essential microelements in the immune system. *Int J Immunol* 10:1-4.
- Maccatrozzo L, Bargelloni L, Cardazzo B, et al., 2001. A novel second myostatin gene is present in teleost fish. *Febs Lett* 509:36-40.
- Mahdy OA, Abdel-Maogood SZ, Abdelsalam M, et al., 2024a. A multidisciplinary study on Clinostomum infections in Nile tilapia: micro-morphology, oxidative stress, immunology, and histopathology. *BMC Vet Res* 20:60.
- Mahdy OA, Abdelsalam M and Salem MA, 2023. Molecular characterization and immunological approaches associated with yellow grub trematode (clinostomid) infecting Nile Tilapia. *Aquac Res* 2023:5579508.
- Mahdy OA, Salem MA, Abdelsalam M, et al., 2024b. An innovative approach to control fish-borne zoonotic metacercarial infections in aquaculture by utilizing nanoparticles. *Sci Rep* 14:25307.
- Martins ML, Santos GGD, 2024. Metal nanoparticles in combating fish parasites: an updated overview. Publisher: UFSC/CNPQ/Editor: Maurício Laterça Martins and Gracienhe Gomes dos Santos
- Mawed SA, Marini C, Alagawany M, et al., 2022. Zinc oxide nanoparticles (ZnO-NPs) suppress fertility by activating autophagy, apoptosis, and oxidative stress in the developing oocytes of female zebrafish. *Antioxidants* 11(8), 1567.
- McPherron AC, Lawler AM and Lee SJ, 1997. Regulation of skeletal muscle mass in mice by a new TGF- β superfamily member. *Nature* 387:83-90.
- Mehdi Y, Hornick JL, Istasse L, et al., 2013. Selenium in the environment, metabolism and involvement in body functions. *Molecules* 18:3292-3311.
- Mengarda AC, Silva TC, Silva AS, et al., 2023. Toward anthelmintic drug candidates for toxocarasis: Challenges and recent developments. *Eur J Med Chem* 251:115268.
- Mi X-j, Le H-M, Lee S, et al., 2022. Silymarin-functionalized selenium nanoparticles prevent LPS-induced inflammatory response in RAW264.7 cells through downregulation of the PI3K/Akt/NF- κ B pathway. *ACS omega* 7:42723-42732.
- Moretti I, Ciciliot S, Dyar KA, et al., 2016. MRF4 negatively regulates adult skeletal muscle growth by repressing MEF2 activity. *Nat Commun* 7:12397.
- Mwainge VM, Ogwai C, Aura CM, et al., 2021. An overview of fish disease and parasite occurrence in the cage culture of *Oreochromis niloticus*: A case study in Lake Victoria, Kenya. *Aquatic Ecosystem Health Manage* 24:43-55.
- Ortuste Quiroga HP, Ganassi M, et al., 2022. Fine-tuning of Piezo1 expression and activity ensures efficient myoblast fusion during skeletal myogenesis. *Cells* 11:393.
- Otero-Tarrazón A, Perelló-Amorós M, Jorge-Pedraza V, et al., 2023. Muscle regeneration in gilthead sea bream: Implications of endocrine and local regulatory factors and the crosstalk with bone. *Front Endocrinol* 14:1101356.
- Parrino V, Cappello T, Costa G, et al., 2018. Comparative study of haematology of two teleost fish (*Mugil cephalus* and *Carassius auratus*) from different environments and feeding habits. *Eur Zool J* 85:193-199.
- Patruno M, Sivieri S, Poltronieri C, et al., 2008. Real-time polymerase chain reaction, in situ hybridization and immunohistochemical localization of insulin-like growth factor-1 and myostatin during development of *Dicentrarchus labrax* (Pisces: Osteichthyes). *Cell Tissue Res* 331:643-658.
- Pawłowska M, Miła-Kierzenkowska C, Szczepielniak J, et al., 2023. Oxidative stress in parasitic diseases—Reactive oxygen species as mediators of interactions between the host and the parasites. *Antioxidants* 13:38.
- Ponnampalam EN, Kiani A, Santhiravel S, et al., 2022. The importance of dietary antioxidants on oxidative stress, meat and milk production, and their preservative aspects in farm animals: Antioxidant action, animal health, and product quality—Invited review. *Animals* 12:3279.
- Qiao L, Chen Y, Song X, et al., 2022. Selenium nanoparticles-enriched *Lactobacillus casei* ATCC 393 prevents cognitive dysfunction in mice through modulating microbiota-gut-brain axis. *Int J Nanomed* 17:4807.
- Radwan M, El-Sharkawy MA, Alabssawy AN, et al., 2023. The synergy between serious parasitic pathogens and bacterial infestation in the cultured Nile tilapia (*Oreochromis niloticus*): a severe threat to fish immunity, causing mass mortality and significant economic losses. *Aquac Int* 31:2421-2449.
- Radwan M, Shehata S, Abdelhadi Y, et al., 2021. Histopathological, Haematological and Biochemical Indices of *Clarias gariepinus* (Burchell, 1822) parasitized by endoparasitic fauna in fish farm of the Northeastern Egypt. *Turk J Fish Aquat Sci* 21:465-478.
- Ralliére C, Jagot S, Sabin N, et al., 2023. Dynamics of pax7 expression during development, muscle regeneration, and in vitro differentiation of satellite cells in the trout. *BioRxiv:2023.2007.2019.549701*.
- Rathore SS, Hanumappa SM, Yusufzai SI, et al., 2023. Dietary administration of engineered nano-selenium and vitamin C ameliorates immune response, nutritional physiology, oxidative stress, and resistance against *Aeromonas hydrophila* in Nile tilapia (*Oreochromis niloticus*). *Biol Trace Elem Res* 201:4079-4092.

- Rathore SS, Murthy HS, Mamun MAA, et al., 2021. Nano-selenium supplementation to ameliorate nutrition physiology, immune response, antioxidant system and disease resistance against *Aeromonas hydrophila* in monosex Nile tilapia (*Oreochromis niloticus*). *Biol Trace Elem Res* 199:3073-3088.
- Rbbani G, Murshed R, Siriyappagouder P, et al., 2024. Embryonic temperature has long-term effects on muscle circRNA expression and somatic growth in Nile tilapia. *Front Cell Dev Biol* 12:1369758.
- Reda R, Khalil AA, Elhady M, et al., 2024. Anti-parasitic activity of garlic (*Allium sativum*) and onion (*Allium cepa*) extracts against *Dactylogyrus* spp. (Monogenean) in Nile tilapia (*Oreochromis niloticus*): Hematology, immune response, histopathological investigation, and inflammatory cytokine genes of gills. *BMC Vet Res* 20:334.
- Reda FM, Alagawany M, Salah AS, et al., 2024. Biological selenium nanoparticles in quail nutrition: biosynthesis and its impact on performance, carcass, blood chemistry, and cecal microbiota. *Biol Trace Elem Res* 202(9): 4191-4202.
- Rigos G, Padros F, Golomazou E, et al., 2024. Antiparasitic approaches and strategies in European aquaculture, with emphasis on Mediterranean marine finfish farming: Present scenarios and future visions. *Rev Aquac* 16:622-643.
- Roberts SB, Goetz FV, 2001. Differential skeletal muscle expression of myostatin across teleost species, and the isolation of multiple myostatin isoforms. *Febs Lett* 491:212-216.
- Ruan RuiXia RR, Yu JuHua YJ, Li HongXia LH, et al., 2011. Isolation of two growth hormone receptor genes and SNPs associated with body weight in GIFT strain tilapia *Oreochromis niloticus*. *Chin J Zool* 46 (3) 37-46.
- Saad AM, Sitohy MZ, Ahmed AI, et al., 2021. Biochemical and functional characterization of kidney bean protein alcalase-hydrolysates and their preservative action on stored chicken meat. *Molecules* 26:4690.
- Saad AM, Sitohy MZ, Sultan-Alolama MI, et al., 2022. Green nanotechnology for controlling bacterial load and heavy metal accumulation in Nile tilapia fish using biological selenium nanoparticles biosynthesized by *Bacillus subtilis* AS12. *Front Microbiol* 13, 1015613.
- Satheeshkumar P, Ananthan G, Kumar DS, et al., 2012. Haematology and biochemical parameters of different feeding behaviour of teleost fishes from Vellar estuary, India. *Comp Clin Pathol* 21:1187-1191.
- Sedyaw P, Bhatkar V, 2024. A review on application of aquaculture drugs for sustainable aquaculture. *Eur J Dev Res* 14:66685-66690.
- Sentkowska A, Pyrzyńska K, 2023. Antioxidant properties of selenium nanoparticles synthesized using tea and herb water extracts. *Appl Sci* 13:1071.
- Sheikh S, Ghoghhi F, Ghelichi A, et al., 2024. Dietary effects of selenium nanoparticles on growth performance, survival rate, chemical composition, and muscle bioaccumulation of Nile tilapia (*Oreochromis niloticus*). *Biol Trace Elem Res* 202:2308-2313.
- Shinn AP, Avenant-Oldewage A, Bondad-Reantaso MG, et al., 2023. A global review of problematic and pathogenic parasites of farmed tilapia. *Rev Aquac* 15:92-153.
- Song J, Zhou J, Li X, et al., 2022. Nano-selenium stabilized by Konjac Glucomannan and its biological activity in vitro. *LWT-Food Sci Technol* 161:113289.
- Song X, Chen Y, Sun H, et al., 2021. Physicochemical stability and functional properties of selenium nanoparticles stabilized by chitosan, carrageenan, and gum Arabic. *Carbohydr Polym* 255:117379.
- Sun Y, Yu X, Tong J, 2012. Polymorphisms in myostatin gene and associations with growth traits in the common carp (*Cyprinus carpio* L.). *Int J Mol Sci* 13:14956-14961.
- Thagfan FA, Baazaoui N, Alamoudi SA, et al., 2025. Eco-friendly zinc nanoparticles biosynthesized by *Lactobacillus casei* as alternative anticoccidial agent ameliorate *Eimeria tenella* infection in broiler chickens: Impact on oxidative stress, intestinal health, growth performance, and gut microbiota. *Results Eng* 26:104929.
- Ugli TFM, Ergashovich YK, Abdukhalilovich SA, et al., 2025. Synthesis, characterization, and cytotoxic activity of stable selenium nanoparticles-incorporated carboxymethylcellulose solution. *Polym Adv Technol* 36:e70232.
- Vijayaram S, Ghafarifarsani H, Vuppala S, et al., 2025. Selenium nanoparticles: revolutionizing nutrient enhancement in aquaculture—a review. *Biol Trace Elem Res* 203:442-453.
- Wang L, Zhang D, Li S, et al., 2021. Dietary selenium promotes somatic growth of rainbow trout (*Oncorhynchus mykiss*) by accelerating the hypertrophic growth of white muscle. *Biol Trace Elem Res* 199:2000-2011.
- Wang R, Chen F, Chen Q, et al., 2022. MyoD is a 3D genome structure organizer for muscle cell identity. *Nat Commun* 13:205.
- Yang CG, Wang XL, Tian J, et al., 2013. Evaluation of reference genes for quantitative real-time RT-PCR analysis of gene expression in Nile tilapia (*Oreochromis niloticus*). *Gene* 527:183-192.
- Yazhiniprabha M, Gopi N, Mahboob S, et al., 2022. The dietary supplementation of zinc oxide and selenium nanoparticles enhance the immune response in freshwater fish *Oreochromis mossambicus* against aquatic pathogen *Aeromonas hydrophila*. *J Trace Elem Med Biol* 69:126878.
- Yildiz HY, Yilmaz BH, 2024. Dietary citric acid decreased the theront number of *Cryptocaryon irritans* (Ciliata) in seawater-adapted tilapia (*Oreochromis niloticus*). *J Fish Dis* 47:e13881.
- Zou G, Zhu Y, Liang H, et al., 2015. Association of pituitary adenylate cyclase-activating polypeptide and myogenic factor 6 genes with growth traits in Nile tilapia (*Oreochromis niloticus*). *Aquacult Int* 23:1217-1225.